R71-16
30 April 1971

FIRST QUARTERLY TECHNICAL REPORT
(1 January – 31 March 1971)

USE OF ELECTRON BEAM GUN FOR HARD ROCK EXCAVATION

Submitted to:

U.S. Department of Interior
Bureau of Mines
Twin Cities Mining Research Center
Twin Cities, Minnesota

Contract No. H0110377

Sponsored by

Advanced Research Projects Agency
ARPA Order No. 1578
Program Code 0F010

Westinghouse
Missile Launching & Handling Department
Sunnyvale, California

The views and conclusions contained in this document are those of the authors and should not be interpreted as necessarily representing the official policies, either expressed or implied, of the Advanced Research Projects Agency or the U. S. Government.

Distribution of this document is unlimited.

DISCLAIMER NOTICE

THIS DOCUMENT IS THE BEST QUALITY AVAILABLE.

COPY FURNISHED CONTAINED A SIGNIFICANT NUMBER OF PAGES WHICH DO NOT REPRODUCE LEGIBLY.

UNCLASSIFIED

Security Classification

DOCUMENT CONTROL DATA - R & D

(Security classification of title, body of abstract and indexing annotation must be entered when the overall report is classified)

1. ORIGINATING ACTIVITY *(Corporate author)*
WESTINGHOUSE ELECTRIC CORPORATION
Missile Launching & Handling Department
Hendy Avenue, Sunnyvale, California

2a. REPORT SECURITY CLASSIFICATION
Unclassified

2b. GROUP
---

3. REPORT TITLE
USE OF ELECTRON BEAM GUN FOR HARD ROCK EXCAVATION
—First Quarterly Technical Report

4. DESCRIPTIVE NOTES *(Type of report and inclusive dates)*
Quarterly Technical Report (1 January - 31 March 1971)

5. AUTHOR(S) *(First name, middle initial, last name)*
David R. Nixon; Dr. Berthold W. Schumacher

6. REPORT DATE	7a. TOTAL NO. OF PAGES	7b. NO. OF REFS
30 April 1971	61	9

8a. CONTRACT OR GRANT NO	9a. ORIGINATOR'S REPORT NUMBER(S)
H0110377	
b. PROJECT NO ARPA Order No. 1578	WEC R71-16
c. Program Code 0F10	9b. OTHER REPORT NO(S) *(Any other numbers that may be assigned this report)*
d	

10. DISTRIBUTION STATEMENT
Distribution of this document is unlimited.

11. SUPPLEMENTARY NOTES	12. SPONSORING MILITARY ACTIVITY
	Advanced Research Projects Agency Washington, D. C. 20301

13. ABSTRACT

A 36 kW electron beam gun is being readied for field test (not funded by the contract). A design has been developed for the gun support or carriage, and preliminary fabrication has started. The Logan Quarry in Aromas, California, has been tentatively selected as the field test site. A mathematical model that can describe the piercing of the rock by the electron beam and subsequently produced thermal stresses is under development. Laboratory tests involving vertical piercing with a 9 kW gun have been conducted in gabbro, sandstone, and quartzite. The results are in good agreement with the prediction of the cavity model developed in theoretical studies.

DD FORM 1473

UNCLASSIFIED

Security Classification

14 KEY WORDS	LINK A		LINK B		LINK C	
	ROLE	WT	ROLE	WT	ROLE	WT
Electron Beam						
Tunneling						
Mining						
Rocks						
Minerals						
Excavation						
Fracture Mechanics						
Evaporation						
Melting						
Thermal Stress						

Distribution of this document is unlimited.

R71-16
30 April 1971

FIRST QUARTERLY TECHNICAL REPORT
(1 January—31 March 1971)

USE OF ELECTRON BEAM GUN FOR HARD ROCK EXCAVATION

Contract No. H0110377

ARPA Order No. 1578
Program Code 0F010

Effective Date of Contract: 11 December 1970
Contract Expiration Date: 10 December 1971
Amount of Contract: $240,000 (CPFF)

Principal Investigator: David R. Nixon
(408) 735-2271

Project Scientist: Dr. B. W. Schumacher
(412) 256-3522

WESTINGHOUSE ELECTRIC CORPORATION
Missile Launching & Handling Department
Sunnyvale, California

Distribution of this document is unlimited.

FOREWORD

This Quarterly Technical Report, covering the period 1 January—31 March 1971, was prepared by the Westinghouse Electric Corporation.

The research reported in this document is supported by the Advanced Research Projects Agency of the Department of Defense and is monitored by the Bureau of Mines under Contract No. H0110377.

CONTENTS

ILLUSTRATIONS

TABLE

SUMMARY

PURPOSE

Westinghouse is seeking field operating data with which to verify and extend theoretical and laboratory data on the feasibility of employing the electron beam gun to satisfy the needs for removal of hard rock. These practical data will provide initial definition of equipment configuration and applicable modes of operation.

TECHNICAL PROBLEMS

Support Equipment. Westinghouse is modifying its existing 36-kW electron beam gun and will provide support equipment necessary for field operation.

Field Tests. This program involves the use of the 36-kW electron beam gun to determine whether laboratory test data on melting rates, breakage, mechanisms, etc, can be extrapolated to predict field performance. The field site being selected will provide working faces representative of a large, relatively unfractured rock mass. During field tests, Westinghouse will determine the techniques and procedures, such as cutting pattern, gun tracing speed, and method of cut, required to produce the optimum excavation rate.

Theoretical Studies. Westinghouse will study the effects of different heating geometries and heating rates on stress distribution patterns and associated breakage phenomena. Westinghouse will also attempt to develop theoretical models for an optimum mode of operation.

Laboratory Tests. Westinghouse will conduct laboratory tests to support theoretical work and field experiments and to extend the use of the electron beam gun to different rock types.

Systems Analysis Study. Westinghouse will evaluate the feasibility of developing a hard-rock excavation system using the electron beam gun as the prime source of power for rock fragmentation.

TECHNICAL RESULTS

This report covers effort performed during the first three months of the contract. Work was performed in four of the five areas summarized above; the systems analysis study will not become active until the field test effort has been completed and evaluated. A sixth area (not included in the contract) is the completion of the 36-kW electron beam gun and its conversion from a laboratory model to a field test version.

Support Equipment. A design has been developed for the gun support or carriage, and preliminary fabrication work has begun in the manufacturing phase of the task (see Section 2). The gun carriage design is basically a four-wheeled trailer with a movable superstructure, which supports, manipulates, and positions the gun during cutting operations. The motions required are powered and controlled with an electro-hydraulic drive system. In addition to the gun, the carriage also supports its hydraulic system (motor, pumps, reservoir, etc.) and the gun's upper-stage vacuum system. The carriage design specification and general assembly drawings are included as Appendix A.

Field Tests. Field test activity to date has consisted primarily of site review and selection (see Section 3). Some aspects considered desirable in a test site are: (a) relatively hard rock, (b) large, relatively unfractured rock mass, (c) several feet of overburden above the cutting site, (d) large floor area to minimize difficulty of operation, and (e) availability of utilities, security, living quarters, etc. Because of the additional complications presented in underground operation, e.g., limited space and possible environmental problems, Westinghouse has concentrated on open quarry sites for the first field tests. Several quarries and one mine have been reviewed. As a result, the Logan Quarry in Aromas, California, which is near Watsonville, has been tentatively selected as a site. Other tasks being pursued in the field test phase are the specification for and design of radiation shielding for the site.

Theoretical Studies. A mathematical model that can describe the piercing of the rock by the electron beam and the subsequently produced thermal stresses is under development (see Section 4). In its present stage, it can describe the initial phases of the piercing process very well. The model results are in good agreement with the results of a series of laboratory tests carried out expressly to check the validity of the theoretical approach.

Laboratory Tests. Laboratory experiments involving vertical piercing with a 9-kW gun have been conducted in test specimens of gabbro, sandstone, and quartzite (see Section 5). These experiments have yielded results that are in good agreement with the predictions of the cavity model, developed in the theoretical studies.

DoD IMPLICATIONS

The primary implications within the DoD sphere of operations, which could result from this field test program, may be summarized as follows: The potential to satisfy any need for the fragmentation and removal of hard rock from a predetermined location without degrading the structural capabilities of the parent rock from which the removal was accomplished.

With an appropriate development program completed, one can envision the application of an electron beam gun to rock-removal systems for programs such as:

Sanguine
Cheyenne Mountain
Minuteman
Safeguard
AEC testing

and quite probably a reasonable number of applications not yet recognizable.

However, it is important to note that considerable product (system) development will be required following the assumed successful field tests before a really productive system can be delivered.

IMPLICATIONS FOR FURTHER RESEARCH AND DEVELOPMENT

It is Westinghouse's belief that the current field test program will demonstrate the state-of-the-art potential of the electron beam gun as applied to hard-rock fragmentation. Based on the results of these tests, additional research and development effort can be envisioned in areas such as:

1. Increase in power or increase in electron acceleration voltage.

2. Effectiveness of the gun on various kinds of rock and rock formations.

3. Analysis of potential environmental problems, e.g.,
   a. Heat production
   b. Radiation
   c. Gases.

4. Improved knowledge of rock mechanics.

These typical areas of continuing investigation will augment a product development program, which is directed toward defining a realizable system that will satisfy government and industrial needs for hard-rock removal.

1. INTRODUCTION

During the past three years, laboratory tests conducted by Westinghouse have shown that the electron beam gun (EBG) may be a promising tool for use in hard-rock excavation (Refs. 1 and 2)*. These tests have been conducted on small, unconstrained, laboratory test specimens weighing a few hundred pounds. Under the present contract, field tests are to be conducted to study the electron beam process on a semi-infinite, constrained rock mass, such as might be encountered in mining or tunneling operations.

The objectives of the electron beam gun evaluation program are:

1. To obtain field operating data.

2. To determine the effectiveness and economic feasibility of the electron beam gun compared with conventional methods of hard rock excavation.

3. To determine practical optimums for equipment configuration and modes of operation.

In support of the foregoing effort, laboratory experiments and theoretical studies will be conducted to compute and if possible, to predict, the thermal stresses and the resultant rock fragmentation for various cutting strategies and electron beam parameters in different types of rock.

*See list of references in Appendix B.

2. ELECTRON BEAM GUN AND SUPPORT EQUIPMENT

2.1 ELECTRON GUN AND CONTROLS

The electron gun is the key element in the new rock cutting machine. Electron beam guns for welding in vacuum and in the atmosphere have been built by Westinghouse for some time and are described in References 3 and 4. Therefore, only the main features will be described here. The electron beam enters the atmosphere through a series of apertures of diameter 0.15 cm to 0.6 cm, which separate a series of differentially pumped vacuum chambers that, are connected to a series of vacuum pumps. In successive chambers an increasingly better vacuum is achieved until in the electron gun chamber proper, a high vacuum of 10^{-5} Torr is attained. This arrangement is shown schematically in Figure 2-1, taken from a previous publication. Before the beam enters the atmosphere, it passes through an overpressure chamber at a pressure of about 1.2 to 2 atmospheres, which also produces an effluent of gas from the gun muzzle into the atmosphere. This prevents debris from being sucked into the gun. The overpressure gas can be air, but it is preferable to use a gas of a low atomic number, such as helium. The beam scatters less in helium than in air, since the ratio of scattering cross sections is 20:1. Therefore, with effluent helium, the beam maintains its power density for a longer distance in front of the gun muzzle. The major part of the helium, which is pumped through the vacuum system, is collected and recycled. This keeps the total consumption of helium to a moderate amount. At a later time, the helium may be replaced by a flame of burning gas that will reduce beam scattering because of the lower density of the hot gas.

The beam is usually focused at the exit orifice of the gun to keep this orifice as small as possible. It has been found however, that it may be advantageous to focus the beam somewhat beyond the gun muzzle (see Figure 5-5). This requires using a larger beam exit orifice, because the beam diameter ahead of the focus is larger; the new 36 kW gun has sufficient pumping capacity to accommodate such larger orifices.

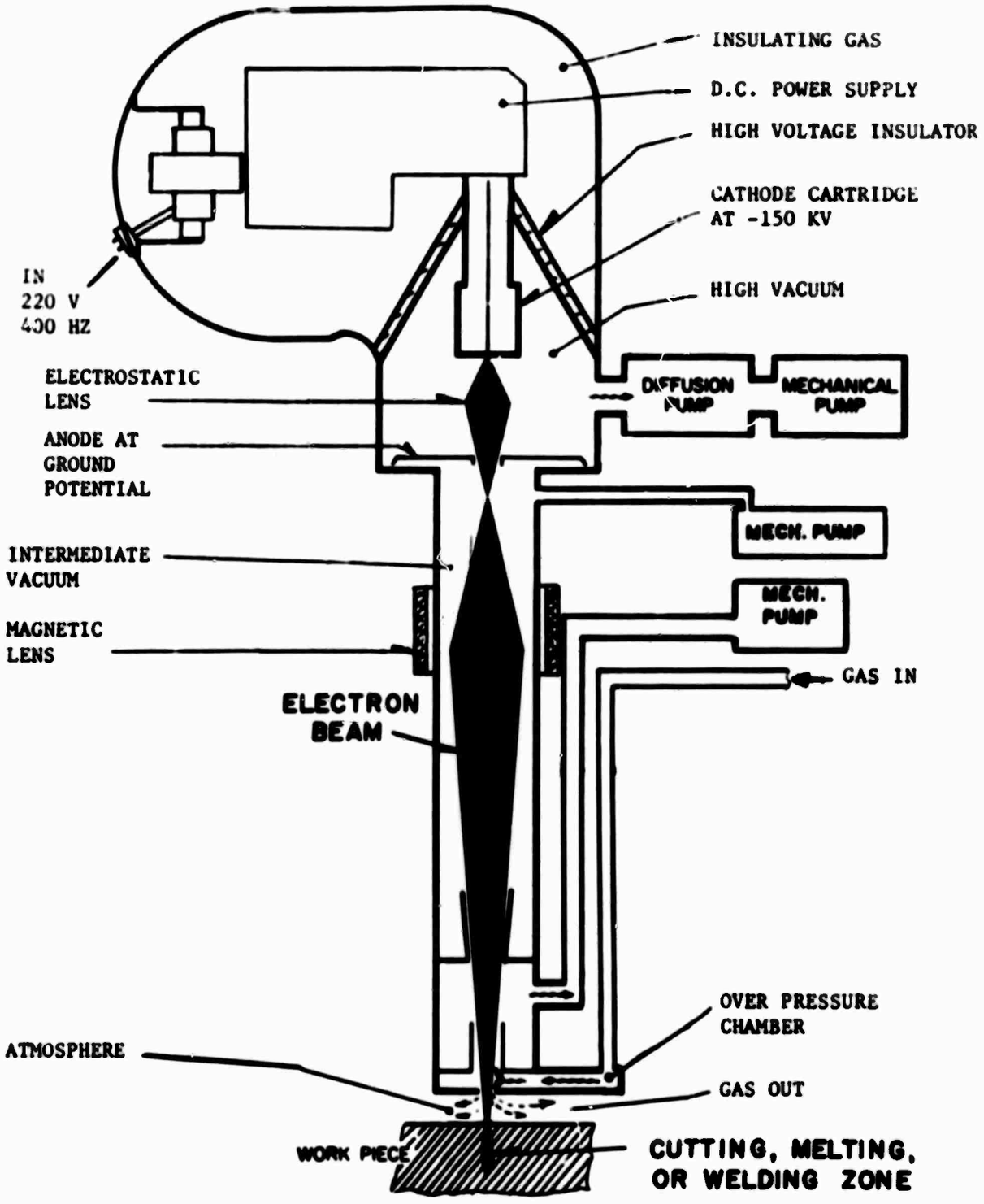

Figure 2-1. Schematic of Nonvacuum Electron Beam Gun

The electron beam gun (but not the gun support system) to be used in the field tests is shown in Figure 2-2. The machine has three single-phase power supplies rated 12 kW each. They are connected to a three-phase motor generator set and together will yield 36 kW of dc power at 150 kV. The beam exit orifice of this machine is located at the end of a 4-foot-long duct section. In the photograph, the machine is tilted so that the beam exit orifice points towards the floor. The machine can be rotated to shoot the beam from a nearly vertical to a horizontal direction. But, in principle, there are no limits as to the orientation of the electron gun. The gun and power supply package as such do not contain any moving parts (if one disregards the drives for vacuum valves, etc.). The total length is 9 feet; the width, 4 feet; and the height, 4-1/2 feet. This package weighs approximately 1500 pounds. It is connected to a set of small Rootes-type vacuum pumps by flexible, 3-inch-diameter vacuum hoses, which must be kept shorter than 12 feet. A further connection to a set of mechanical pumps is made by two 3-inch hoses, which may be 30 to 60 feet long. A plan view layout of this system is shown in Figure 2-3. The Beam Control Console for starting up and monitoring the performance of the machine can also be seen in Figure 2-2. This console must be within 200 feet of the machine, which is the present length of the cables. Another 200-foot cable goes to the man who performs the actual cutting operation and who needs nothing but an ON/OFF button for the beam and, of course, the gun positioning controls.

A more detailed description of the electron gun itself will be given with the final report.

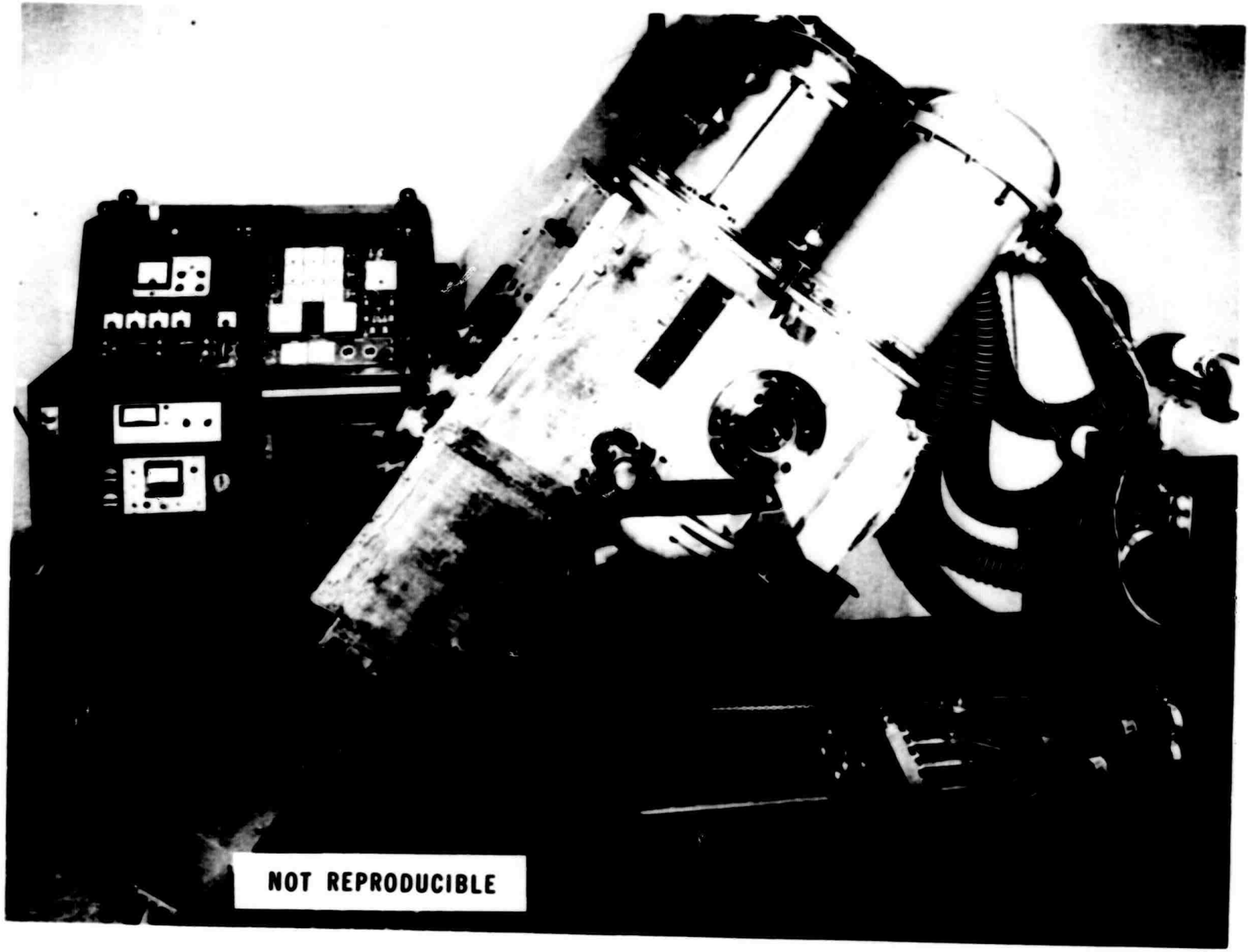

Figure 2-2. New Electron Beam Gun for Field Tests on Auxiliary Stand

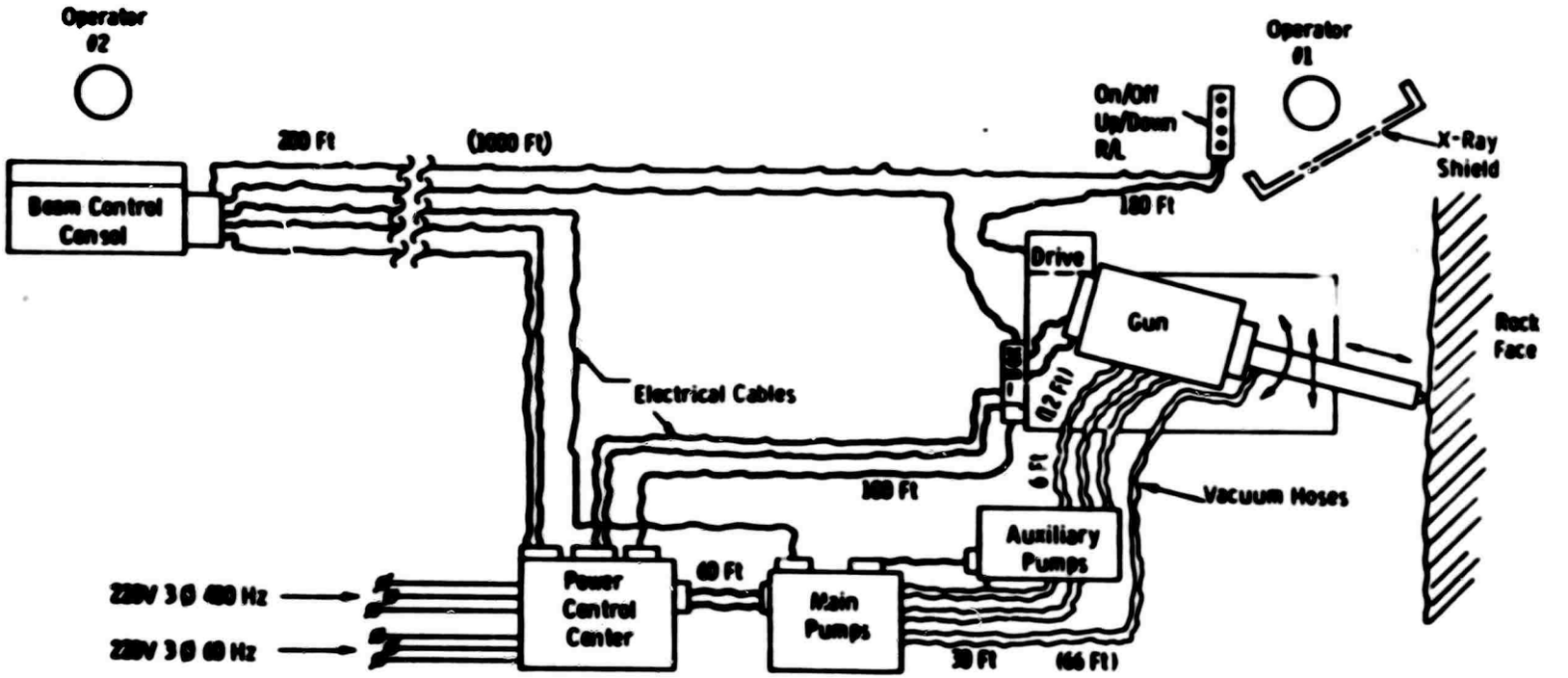

Figure 2-3. Plan View of Complete Field Test Setup

2.2 SUPPORT EQUIPMENT

Support equipment for the electron beam gun is comprised of the electrical power supply system, the gun vacuum system, and the gun carriage. The electrical and vacuum equipment existed as laboratory equipment prior to work on the field test program, so the principal task in this area is the design and manufacture of a carriage to support, position, and manipulate the gun during field test operations. The design task is now about 90 percent complete, with only a few details remaining to be resolved. Fabrication of the carriage structure has begun, and it is expected to be completed by late May 1971.

The carriage is designed to permit working on vertical rock face approximately 8 feet high by 8 feet wide. It has the capability to move the gun in the horizontal (X-axis) and vertical (Y-axis) directions parallel to the rock face and in the horizontal direction perpendicular to the rock face (Z-axis) to compensate for irregularities in the rock surface. The attitude of the gun relative to the rock face is also variable as the carriage can rotate the gun in the horizontal (yaw) and vertical (pitch) planes. (A more complete description of the carriage is given in the carriage design specification, Appendix A of this report.)

2.2.1 Design Description *

The initial design concept consisted of a two-wheeled trailer, which provides the basic carriage, and several movable structures mounted on the trailer, which permit the motions previously described. A rectangular frame is contained within the trailer frame and is supported by trolley wheels that ride on the longitudinal members of the trailer. This wheeled box frame provides 30 inches of Z-axis motion. A second rectangular frame (the X-axis frame) is contained within the Z-axis frame and is similarly supported by trolley wheels, which ride on the transverse members of the Z-axis frame. The X-axis frame permits up to 36 inches of motion in the

*See Appendix A for the carriage assembly drawings.

X-axis direction. A thrust bearing is mounted on the X-axis frame and supports the carriage superstructure. This superstructure/thrust bearing combination results in a turntable that permits rotation in the yaw mode. The superstructure is comprised of two vertical members, which support and guide the gun mount during motion in the Y-axis direction. The gun mount, itself, is a 2-inch-diameter shaft that rotates and thereby provides the pitch rotation capability. The ends of the pitch shaft are supported by bearings incorporated in the Y-axis guides, which move vertically in the aforementioned vertical members.

The initial concept used a roller chain drive system, powered by dc variable speed gearmotors. This system was selected because (1) the small power requirements would result in a relatively low cost drive system, (2) most components appeared to be available as "off-the-shelf" hardware, (3) the ability of roller chain systems to function at low speed in dirty environments with minimum of maintenance is a desirable feature, and (4) the speed control capability of a dc drive system was attractive. Initial design layout work was done using the foregoing dc motor/roller chain system.

At this stage in the design task, it became apparent that the power requirements for pitch rotation had been underestimated and that the low speeds required were beyond the reduction capability of most standard gearmotors. At this point, the low-cost advantage of this drive system ceased to exist as the estimated cost of the drive system was over $4000. Alternate systems were then explored with the final selection being the hydraulic system/roller chain combination shown Appendix A. This system has hydraulic cylinders and rotary actuators for power transmission and roller chains as mechanical synchronizing devices. It sacrifices the remote speed control capability of the dc motor system but has other advantages, such as (1) lower cost (about $2500), (2) buffering provided by the cylinders (i.e., prevent free fall of components) in the event of a mechanical failure, and (3) good reliability. The speed control is retained through the use of variable flow control valves for all motions, although speed

changes must now be accomplished by changing valve settings on the carriage. The remote speed control feature could be regained through the use of servo valves, but Westinghouse feels that a servo control system is more sophisticated than is required for field test operations.

3. FIELD TESTS

Effort in the area of field tests has been limited toward (1) review and selection of test sites, (2) the development of site support equipment such as radiation shielding, and (3) registration of the electron beam gun with the California State Department of Public Health as a radiation producing machine.

3.1 TEST SITE SELECTION

A meeting was held at the U. S. Bureau of Mines Twin Cities Research Center on 25 January 1971 to discuss various aspects of test sites. With this discussion in mind, Westinghouse began to review candidate test sites. Because of the complications that might be encountered in an underground mine site, such as limited access and space and the possibility of environmental problems (heat, gases, etc.), Westinghouse has concentrated on open quarry sites for the first field tests. Some of the aspects considered as desirable site features are the following:

1. Geologic considerations
   a. Relatively hard rock type
   b. Large, relatively unfractured, constrained rock mass
   c. Rock surface relatively unweathered
   d. Several feet of overburden above test location
2. Facility considerations
   a. Availability of utilities, communications, security
   b. Availability of acceptable security arrangements
   c. Safety requirements: proximity to medical facilities and X-ray film badge service.

d. Availability of large open work area around test site

e. Proximity to Westinghouse Sunnyvale, California

f. Availability of accommodations for site personnel

g. Climate: minimal chance for precipitation during the four- to six-week test period.

3. Site support considerations

a. Availability of skilled and unskilled labor

b. Availability of support equipment such as cranes, welding equipment, earthmoving equipment, etc.

With the foregoing criteria in mind, Westinghouse has reviewed 12 quarry sites and 1 mine site. The mine, in Albuquerque, New Mexico, is unsuitable for our purposes because of its remote location, the limited access to test faces, and the lack of utilities at the mine site, as well as other reasons. The quarry sites visited ranged from granite quarries in the Rocklin, California area; granodiorite quarries in Madera, California; and granite, limestone, and sandstone quarries in the coast range from Monterey to Marin County (north of San Francisco). Most of the sites reviewed were deemed unsuitable for Westinghouse use for various reasons such as inaccessibility, lack of sufficient rock face and overburden, inadequate utilities available at the site, and high probability of interference with the owners' quarrying operations. However, one site has been located which fulfills most of the site requirements and has therefore been tentatively selected as a field test site.

The selected site is the Logan quartz gabbro quarry in Aromas, California, near Watsonville (see Figure 3-1). This quarry is owned and currently operated by the Granite Rock Company of Aromas, California and is available for electron beam gun test use.

Figure 3-1. View from West Rim of Logan Quartz Gabbro Quarry, Aromas, California, Looking Towards Fractured Rock Area (Arrow indicates proposed working face shown in Figure 3-2.)

It is located about eight miles from Watsonville and is approximately one hour and 15 minutes travel time from the Westinghouse Sunnyvale facility. While not far from Watsonville, the site is relatively isolated and has limited access; thus security should not be a large problem. Utilities are available at the site, and site support equipment and labor are available at cost from the quarry operator.

The quarry itself is approximately one-half mile across and has a flat floor of packed granite sand. The rock walls of the quarry vary from 80 to about 100 feet high and present excellent exposures of unweathered rock, both fractured and relatively unfractured (see Figure 3-2). The rock itself is a hornblende quartz gabbro containing about 10 percent quartz and 35 to 48 percent green hornblende. The Logan formation is described in greater detail by Donald C. Ross in Reference 3.

Figure 3-2. South End of Logan Quarry Showing Rock Face and 100-foot Wall

3.2 RADIATION SHIELDING

During the operation of the electron beam gun, radiation is produced in the form of X rays as a by-product of electron acceleration. The radiation is principally backscatter from the point when the beam strikes the rock. The radiation level at a distance of 1 meter from this point has been estimated at approximately 500 milliroentgens per hour. This radiation is nonresidual and disappears as soon as the beam is shut off. Since the maximum permissible dose for occupational exposure for the whole body is 1.25 roentgens for 13 weeks, shielding is required to protect test personnel and observers. The shielding consists of a lead-lined plywood shed, 20 feet long and 12 feet wide, with one end open. The open end is to be placed against the rock face with the gun and carriage inside the shed. The shed roof is also to be shielded to prevent the occurrence of "sky shine."* Without a shielded roof, the radiation level could increase to an unacceptable level at some distance from the shielded walls. Lead lining is to be 12-pound lead (3/16 inch) on the roof and walls except for the panels closest to the radiation source, which will be 16-pound (1/4 inch) lead. The shed is equipped with leaded glass window for observers and an operator's control booth, which also has leaded glass windows. The structure is portable to the extent on that it can be disassembled and moved from one test location to another.

*Refers to radiation initially directed skyward but deflected back toward earth because of interference with air molecules.

3.3 CALIFORNIA STATE REGISTRATION

As defined by the California Radiation Control Regulations,* the electron beam gun falls into the category of "radiation producing machines" and, therefore, must be registered with the State Department of Public Health. Public Health Department authorities have been contacted regarding registration requirements and registration will be submitted in the near future for operation at the Aromas quarry. State regulations also govern such items as radiation protection, warning sign markings, personnel monitoring, etc. These regulations are currently being studied to assure compliance, but no great degree of difficulty is anticipated in achieving this goal.

*California Radiation Control Regulations, Title 17, Public Health, California Administrative Code, Chapter 5, Subchapter 4, Sections 30100 through 30397.

4. THEORETICAL STUDIES

4.1 PIERCING WITH THE ELECTRON BEAM

A previous study (Ref. 6) has shown that the power density in the electron beam is so high and the thermal diffusivity of all rocks so low, that the rock under the focused beam will melt and vaporize quasi-adiabatically. This means that no energy is lost by heat conduction. Knowing the power density of the beam and the heat of melting and vaporization for the rock, we can therefore immediately determine the melted or vaporized volume per unit time and, hence, the speed with which the rock face will recede under the beam. However, since the electron gun cannot follow (the electron gun being much bigger than the small hole drilled by the beam) the distance between the electron gun muzzle and the rock face will quickly increase. With the increased distance, the beam spreads because of scattering and therefore loses power density. Thus, the rate of melting and/or vaporization will decrease with time. The question is, what is the penetration as a function of time and other factors?

Previous experience has shown that a beam of 9 kW and 150 kV will pierce a hole 2 inches deep within 15 to 30 seconds. The cavity will grow further to a depth of 4 to 6 inches in 2 to 3 minutes. Finally, an equilibrium will be reached where all of the incoming beam energy can be dissipated by the walls of the cavity via heat conductions. From then on, the size of the cavity will remain constant. At this stage, the process is no longer adiabatic, since all the heat flows into the solid rock and raises its temperature. This is desirable, because experience has shown the resulting thermal stresses can then rupture very large blocks of rock.

One would like to have a mathematical model that predicts the penetration of the electron beam as a function of time, as well as the development of the thermal stress field as a function of time, for different types of rock, whose material parameters, such as thermal diffusivity, melting point, etc., will differ. The overall process is obviously very complex,

and to treat it analytically, certain simplifying assumptions must be made. It seems desirable to consider the various phases of the process separately. For instance, the initial penetration of the electron beam, as long as it is adiabatic, can be treated separately. Then after the piercing cavity achieves a certain depth, attention can be switched to the temperature field produced by the heat flow from the walls of this cavity. These walls are covered by a thin layer of molten rock because the electron beam is scattered and hits the walls, and because the vapor condenses there and releases its heat of condensation. Again, simplifying assumptions must be made as to the diameter and the shape of the wall of the cavity, so that we may, for reasons of economy, use certain known analytical solutions of the transient heat flow equation. This is the approach followed and described in the following paragraphs.

With respect to later developments of this theory, we should keep the following points in mind. The above approach of separating the forming-phase of the cavity from the heat flow phase neglects the heat flow into the rock during the time period in which the cavity is actually produced. In principle, the resulting error can be partly compensated for by choosing a zero time for the heat-flow calculation, which is earlier than the point in time where the cavity has reached the assumed depth. On the other hand, heat flow during the first few seconds represents actually very little energy, and where the cavity growth is fastest the speed of the melt-front may even be greater than the speed with which a certain isotherm (temperature-wave) moves into the solid. This is one of the essential features distinguishing the electron beam piercing process from flame jet piercing. A "correct" zero time for the heat flow calculations is therefore difficult to define in any case. Certainly, a correction needs to be applied to the above model for very much longer times of power input, i.e., for piercing times of several minutes, where we already find a significant heat flow into the rock, yet a slow increase in the depth and width of the cavity.

To date such refinements of the calculations have not been considered. Approximate values for the temperature distribution as function of time are obtained by looking at the results of the simplified calculations at various times t_i. If, for these temperature calculations at successive times, t_i, t_{i+1}, etc. cavity sizes are used, which are computed on the basis of "adiabatic" growth in depth, then this yields a kind of time-step picture for the temperature field that may be accurate enough for our purposes. Obviously, if one desires, the model can be improved at the cost of additional computation time.

4.1.1 Mathematical Model for the Initial Piercing Process

To arrive at a relatively simple and tractable mathematical model for the initial phase of the piercing process, the following assumptions are made:

1. Where the center of the beam hits solid rock, the material is melted and vaporized adiabatically; this means heat conduction can be neglected.

2. The heat input required to remove a certain volume of rock, called "heat-of-removal" and designated by H, is assumed to have a definite value. In the first instance it can be assumed H is simply the total heat of vaporization, which for all rocks, has, a value in the neighborhood of 14 kJ/cm^3.

3. Ignoring for the moment the shape of the cavity, we assume that the speed of penetration is determined by the interaction of the most intense part of the beam, i.e., the center, with the solid rock.

4. The power density of the beam in the center is obviously related to the spread of the beam due to scattering. Beam scattering as a function of distance in the gas or the rock vapor is assumed to be known from calculations or from independent measurements.

5. As time progresses the cavity grows deeper and the electron beam must traverse a longer path in the gas or vapor before hitting the bottom of the cavity. Thus, increased scattering of the electrons causes the beam to broaden, to increase its diameter, whereby the power density in the beam center is diminished. (Note that the electron gun itself is much too large to fit into the piercing cavity,

thus it cannot follow the receding rock face; the broadening of the beam leads to a widening of the cavity, which we ignore for the moment.

6. The spread in the beam diameter is not simply a linear function of distance and must be carefully determined or calculated. Accordingly the growth rate of the cavity is not a linear function of time either. Apart from scattering, other factors like the initial angular aperture of the beam can also contribute to the reduction in the power density with distance.

Working with these assumptions it must be kept in mind that the following effects have been neglected:

a. The increase in beam diameter caused by the initial geometric-optical cone angle of the beam. (In the later experiments, but not in the theory, the order of magnitude of this effect has been investigated as shown in Table 5-I.)

b. The change in multiple scattering and therefore beam spread, which is caused by either uniform or irregular heating of the vapors or gas.

c. The energy loss of the individual electrons, estimated to be less than 10 percent, which is caused by collisions with gas molecules.

The next requirement is an analytical expression for the reduction of power density in the beam with distance. According to multiple scattering theory (Ref. 7), a thin electron beam moving in the direction +z and starting at z = 0 has the following Gaussian intensity distribution in the xy-plane at various distances from the muzzle of the gun:

$$j = \frac{I_o}{2\pi\alpha z^3} \exp\left\{ - \frac{x^2+y^2}{2\alpha z^3} \right\} \quad A/cm^2 \qquad (1)$$

Accordingly, the characteristic radius is

$$r_o = \sqrt{\alpha z^3} = \sqrt{\alpha}\, z^{1.5} \quad cm$$

(It increases more than proportionally with distance, i.e., with the 1.5 power.)

The quantity α, which is independent of distance, is given by the expression:

$$\alpha = \frac{2\pi}{3} N \left(\frac{2Ze^2}{pv} \right)^2 \ln\left(\frac{192}{Z^{1/3}} \frac{p}{mc} \right)^{1/2}$$

where N is the number of atoms per cm^3 of the gas through which the beam passes; Z, a weighted average of the atomic numbers of the elements in the gas; e, the electronic charge; p, the relativistic momentum of the electrons; v, the velocity of the electrons; m, the mass of the electron; and c, the speed of light.

Note: Since pv is nearly proportional to the accelerating voltage, and since the logarithmic term is slowly varying, it is apparent that the beam diameter varies almost inversely with the accelerating voltage.

Note: The gas density N varies inversely as the temperature of the gas, which is difficult to predict from theory alone. Accordingly, we used a value of $\alpha = 1.095 \times 10^{-3}$, which was experimentally determined from previous beam profile measurements.

Note: The beam width is also roughly proportional to Z, the atomic number; the composition of the rock (vapor) may therefore have an influence on beam spread.

It should be pointed out that the above equations for beam spread hold only in the so-called multiple scattering regime, which comprises not more than the first 10 percent of the so-called range of the electrons. For larger distances, a Gaussian beam profile is not found anymore; in fact, beam spread and energy dissipation become rather complex. (Ref. 8). In

our present situation, the last 90 percent of range and energy of the electrons fall into the solid rock, and cause its vaporization.

Depth of the Piercing Cavity. The power density at the center of the beam as it strikes the rock face determines the penetration speed and is given according to equation (1) by

$$N^* = j(z)U = \frac{I_o U_o}{2\pi\alpha z^3} = \frac{W_o}{2\pi\alpha z^3} \qquad W/cm^2 \qquad (3)$$

where $W_o = I_o U_o$ is the total beam power.

With reference to the definitions of Figure 4-1, the "rate of growth" of the cavity can be expressed as

$$\frac{dz}{dt} = \frac{1}{H^*} \quad N^* = \frac{1}{H^*} \quad \frac{I_o U_o}{2\pi\alpha z^3} \qquad cm/sec \qquad (4)$$

Upon integration, this yields an expression for the cavity depth as a function of time

$$d = \left\{ \frac{4W_o}{2\alpha\pi H^*} t + z_o^4 \right\}^{1/4} - z_o \qquad (5)$$

where the constant z_o is the location of the rock face before penetration begins, and the cavity depth d is defined as $z-z_o$.

For small values of time, i.e., much less than 1 second at 9 kW depth is directly proportional to time. For large times, the depth is roughly proportional to the 1/4 power of the time. Our experimental data, discussed in Section 5, are mostly from the intermediate region between these two cases. Thus, the depth often appears to vary roughly as the 1/3 power of time.

The influence of the beam voltage enters through the parameter α. Since α is, in the first approximation, inversely proportional to the square of the beam

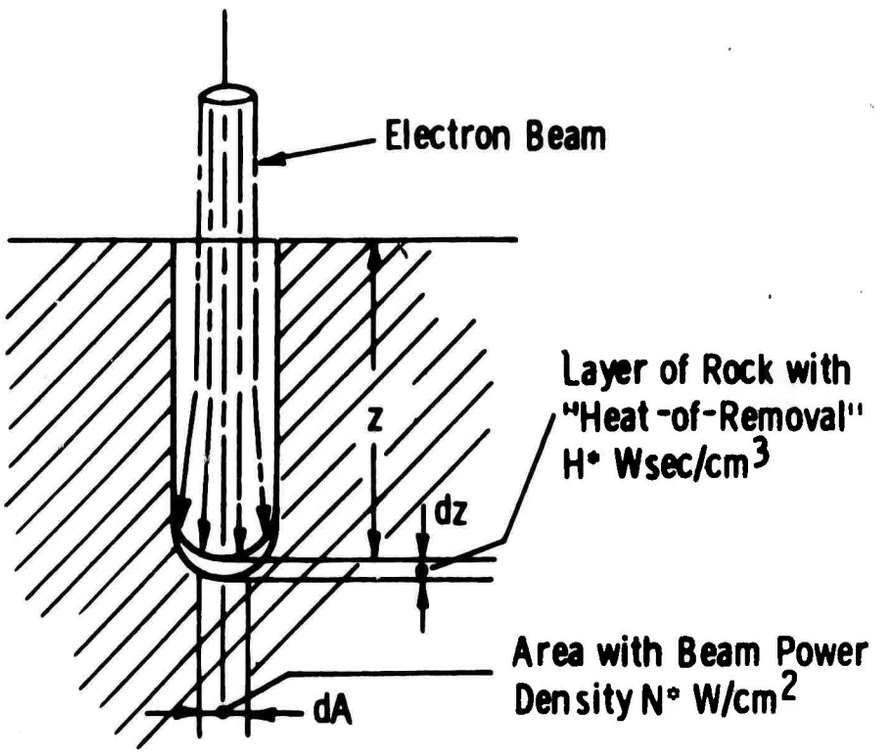

* "Growth-rate" of cavity (assuming adiabatic conditions, i.e. no heat loss due to heat conduction):

$$\frac{dz}{dt} = N^*/H^* \text{ cm/sec}$$

Figure 4-1. Schematic and Definitions for Cavity Growth Rate Calculations

voltage, we see that the rate of growth increases in proportion to the square of the beam voltage. This is a very strong argument to use higher voltages in the rock cutting process, in addition to the fact that the initial radiance of the beam increases with the square of the voltage as well. It must not be concluded from equation (3) that N* is proportional to W_o, since equation (3) represents only the spread of an originally infinitely narrow beam and says nothing about the initial radiance (Ref. 9).

Volume and Shape of the Piercing Cavity. If adiabatic conditions prevailed everywhere the volume of the cavity could be expected to be proportional to the total energy input, but this is not the case and is not even desirable. Where the scattered beam strikes the wall, the rock will melt but will not necessarily be vaporized. Rock vapor from the bottom center of the cavity will condense on the walls and release its heat of vaporization, and cause the walls to melt. From experience, we know the cavity stays relatively narrow, and its walls are at the melting temperature of the rock. We can therefore use the wall of the cavity as a reference surface of known temperature for our subsequent calculations of the temperature distribution in the solid rock.

The penetration rates according to the foregoing theory have been compared to the experiments reported in Section 5. From these and previous experiments, we also know that cavity widths are small compared to their depths. As a first approximation, we assume a cylindrical cavity with a hemispherical bottom. On this basis, we can proceed to calculate the temperature distribution in the surrounding rock as discussed in the following section.

4.2 TEMPERATURE DISTRIBUTION

As a reasonable yet tractable model of the cavity for use in the subsequent temperature and stress analysis, we assume we have a cylindrical cavity, which is deeper than it is wide and is terminated by a hemisphere at its base. For simplicity, we make the additional approximation that the cavity is drilled to its full size instantaneously and that its walls are held at the melting temperature of the rock. We are no longer working under the adiabatic conditions, but on the contrary, we assume that the energy input to the wall is just enough to keep it molten. Such a boundary condition then specifies the amount of energy that flows into the solid rock by heat conduction.

There exist in the literature solutions appropriate for calculating the heat flow through the wall of the cylindrical cavity into the rock. In particular, the transient solution for an infinitely long cylindrical isotherm imbedded in an infinite medium is given by:*

$$T_c(r,t) = (T_m - T_o)\left\{1 - \frac{2}{\pi}\int_0^\infty e^{-\tau u^2}\frac{\left[J_o(u)Y_o(Ru) - Y_o(u)J_o(Ru)\right]}{u\left[J_o^2(u) + Y_o^2(u)\right]}du\right\} + T_c$$

$$\tau \equiv \frac{at}{b^2}$$

$$R \equiv \frac{r}{b}$$

where T_c is the temperature at radial distance r and time t, T_m, the melting temperature; T_o, the ambient temperature; b, the radius of the cylinder; a, the thermal diffusivity; and J_o and Y_o, the first-order Bessel functions of the first- and second-kind, respectively.

---

*See J. C. Jaeger, Journal of Mathematics and Physics, 34 (1955), p. 316.

Similarly, the solution appropriate for the spherical bottom of the cavity is that of a spherical isotherm imbedded in an infinite medium, which is given by:**

$$T_s(r,t) = \frac{T_m - T_o}{R} \left\{ 1 - \text{erf} \frac{R-1}{2\sqrt{\tau}} \right\} + T_o$$

We have completed a computer program that makes use of these two functions to rapidly calculate temperatures for the large number of spatial points used in the finite-element, thermal-stress calculations. In so doing we obtain a good approximation to the correct temperature distribution without resorting to the time-consuming and expensive procedure of solving the time-dependent heat equation numerically. The program uses the cylindrical solution for any point inside the rock whose depth is less than the depth of the cylindrical portion of the cavity. For greater depths, the program assumes that the isotherms conform to smooth (elliptical) curves, which begin at positions dictated by the cylindrical solution and end below the cavity (on the axis defined by the beam) at points dictated by the circular solutions.

Figure 4-2 shows the resulting isotherms for a cavity radius of 0.5 cm, a melting temperature of 1800°C, a thermal diffusivity of 5×10^{-3} cm^2/sec, and an elapsed time of 30 seconds. Obviously this calculation, based on an infinitely long cylinder, is independent of the depth that is assumed for the cavity. The computer program that calculates the temperature distribution can be used with any desired input data, such as melting temperature and thermal diffusivity of the rock, cavity radius, and elapsed time. The two assumptions under which this temperature calculation is valid are, as previously stated, that the cavity is no longer growing so quickly that the melt-front moves with a speed comparable to that of the "heat wave," and that the heat flow occurring during the initial cavity piercing process is negligibly small, because of the short times involved and the rapid progress of the melt-front.

**See H.S. Carslow and J.C. Jaeger, Conduction of Heat in Solids, Second Edition, Oxford University Press, London (1959) p. 247.

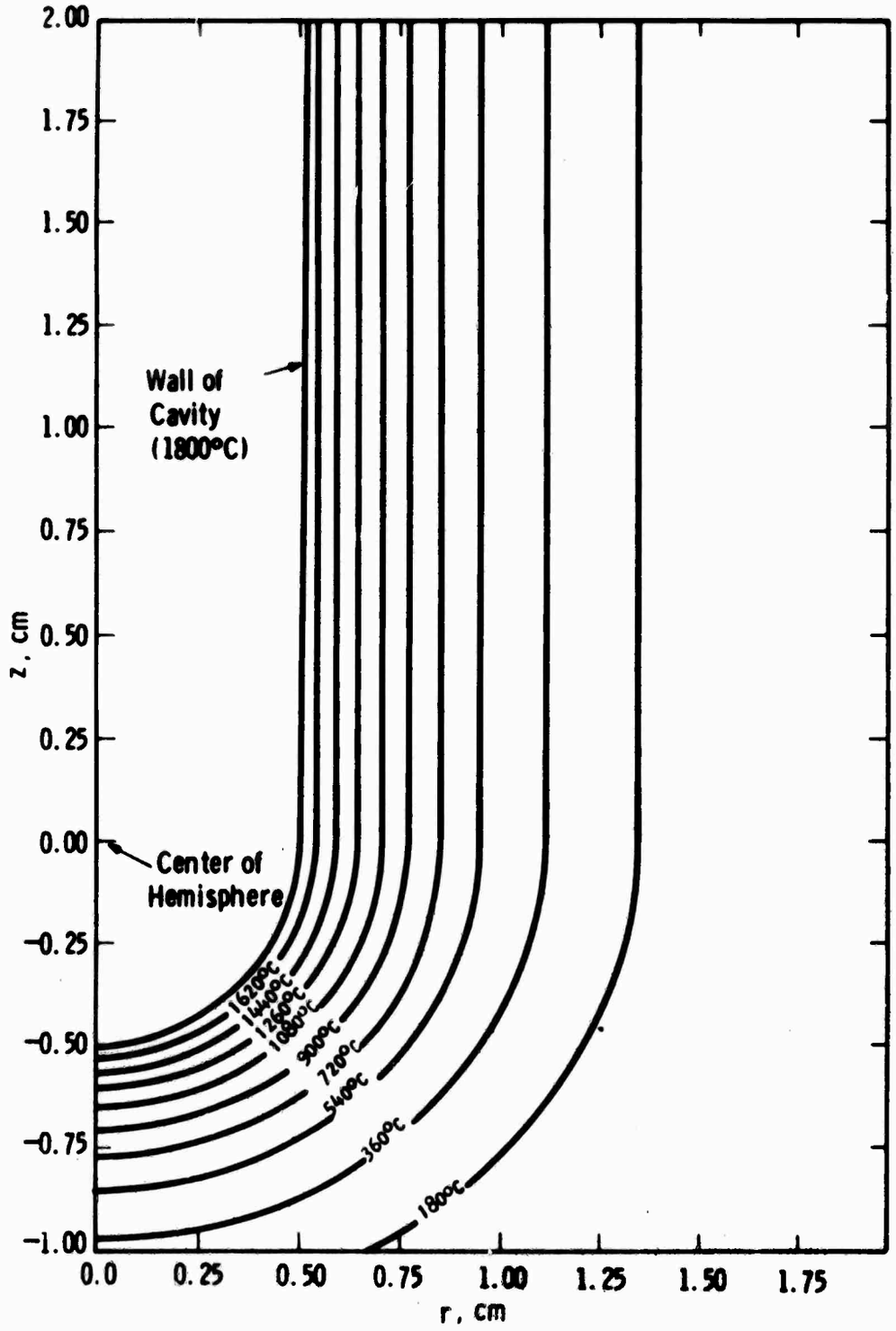

Figure 4-2. Computed Temperature Field for Cavity 2.5 cm Deep, 0.5 cm Diameter, for Rock with Thermal Diffusivity of 0.005 cm^2/sec — 30 Seconds after Cavity Formed and Stationary

4.3 STRESS CALCULATIONS

Work has been started using the above temperature data as input data for some generally available finite-element programs previously developed for thermo-elastic and elastic-plastic stress calculations in various materials. Actual computations have not yet been started.

5. LABORATORY TESTS

5.1 TESTS IN SUPPORT OF THE THEORETICAL STUDIES

To check the penetration rates predicted by equation (5), a few laboratory tests were made with our low-power 9 kW electron gun shooting a beam vertical downwards. In one series of tests, the beam was fired into the top face of a larger piece of rock, as we have done in the past. This has the disadvantage that liquified rock may accumulate at the bottom of the cavity; this factor is not included in our theoretical analysis. Therefore, another set of tests was made in which the beam drilled the cavity very close to a vertical face of the rock. In this case, the cavity breaks through and the liquified rock can flow downwards and out. This corresponds more closely to our theoretical assumptions, and would closely resemble the conditions that we find drilling a cavity with a horizontal beam. Besides, the test is not involuntarily interrupted by the fracture of the rock. Figure 5-1 shows such "cavities" drilled along the smooth face of a block of black gabbro from Oklahoma. The beam, running parallel to the face, hit the top of the sample roughly 0.025 inch from the edge of the rock. Figure 5-2 summarizes the penetration as a function of time as measured in both types of tests.

For the penetration observed along the rock face, the theoretical curve follows the experimental points closely. However, penetration into the body initially proceeds faster, which can be explained by the fact that the vapor temperature is higher in the closed cavity. Therefore, the beam scattering is lower, and the power density remains higher than is assumed in the theory. On the other hand, the penetration into the body levels off after 6 to 7 seconds, most likely because liquid rock has accumulated at the bottom of the cavity. These differences have not been investigated further.

Figure 5-3 shows how our general theory agrees with what we find in different kinds of rock. Cavities were drilled, again along the face of

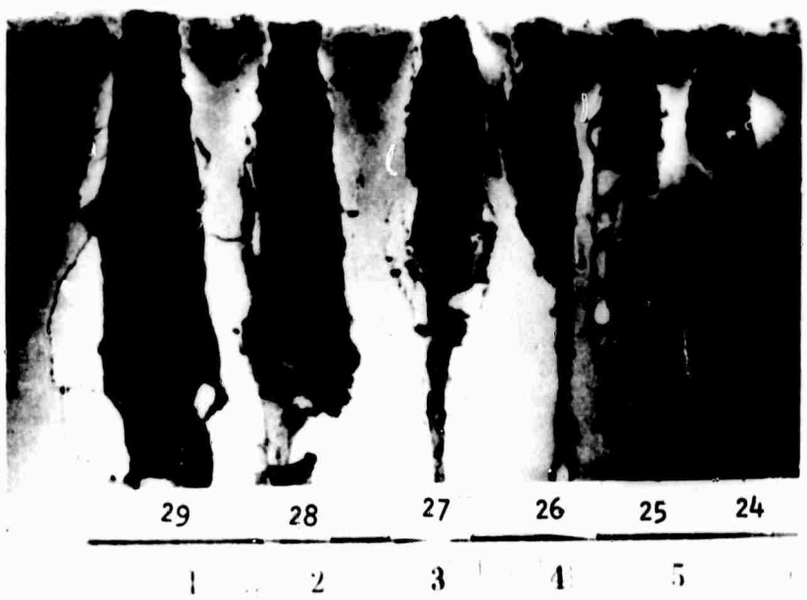

Beam "ON" Time (secs)	32.0	17.9	8.0	4.0	2.1	1.1

Figure 5-1. Cavities Drilled along Smooth Face of Oklahoma Gabbro Sample

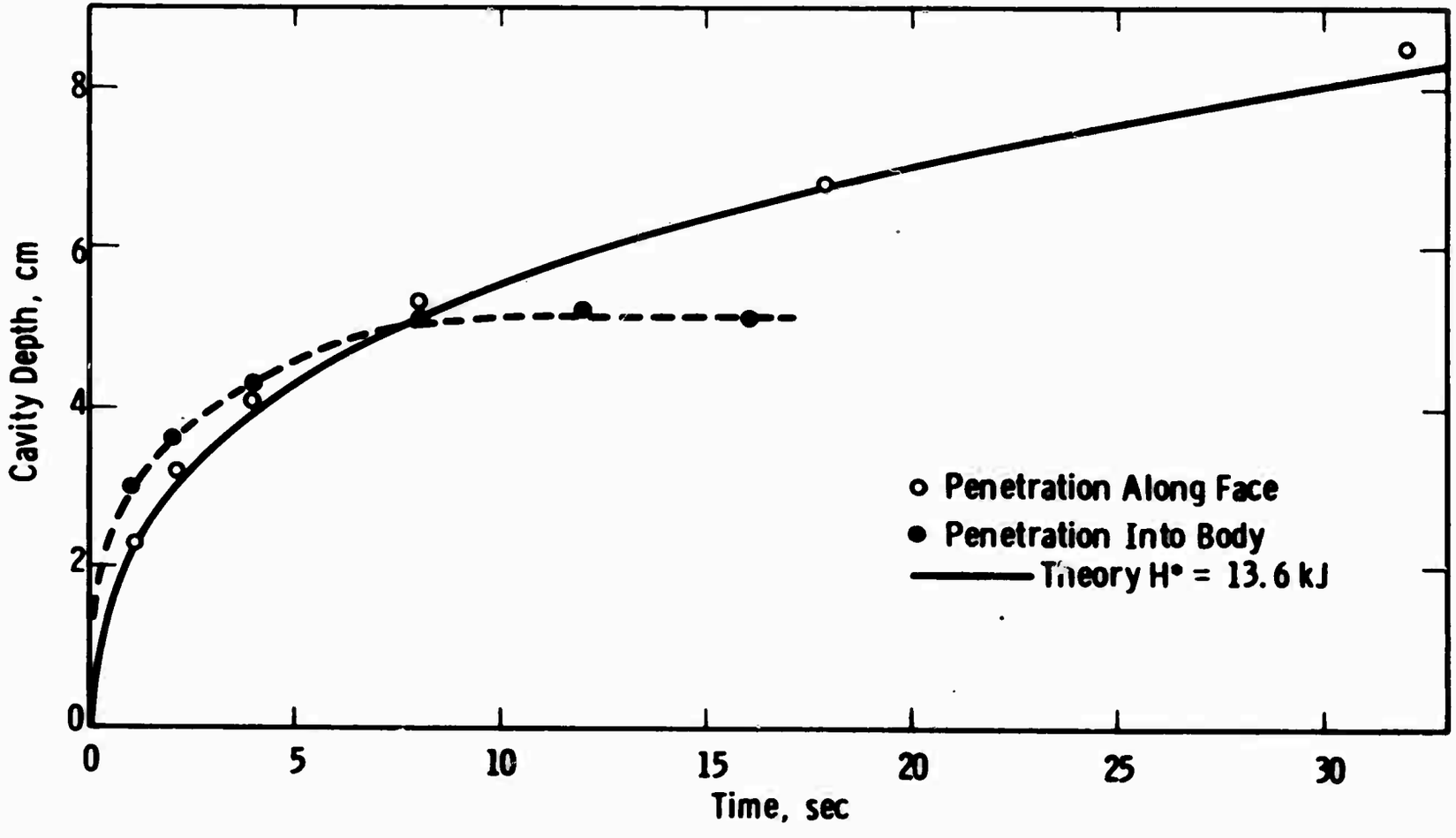

Figure 5-2. Growth of Cavity in Oklahoma Gabbro (Beam Power = 9 kW; 150 kV; Stand-off distance = 1/2 inch)

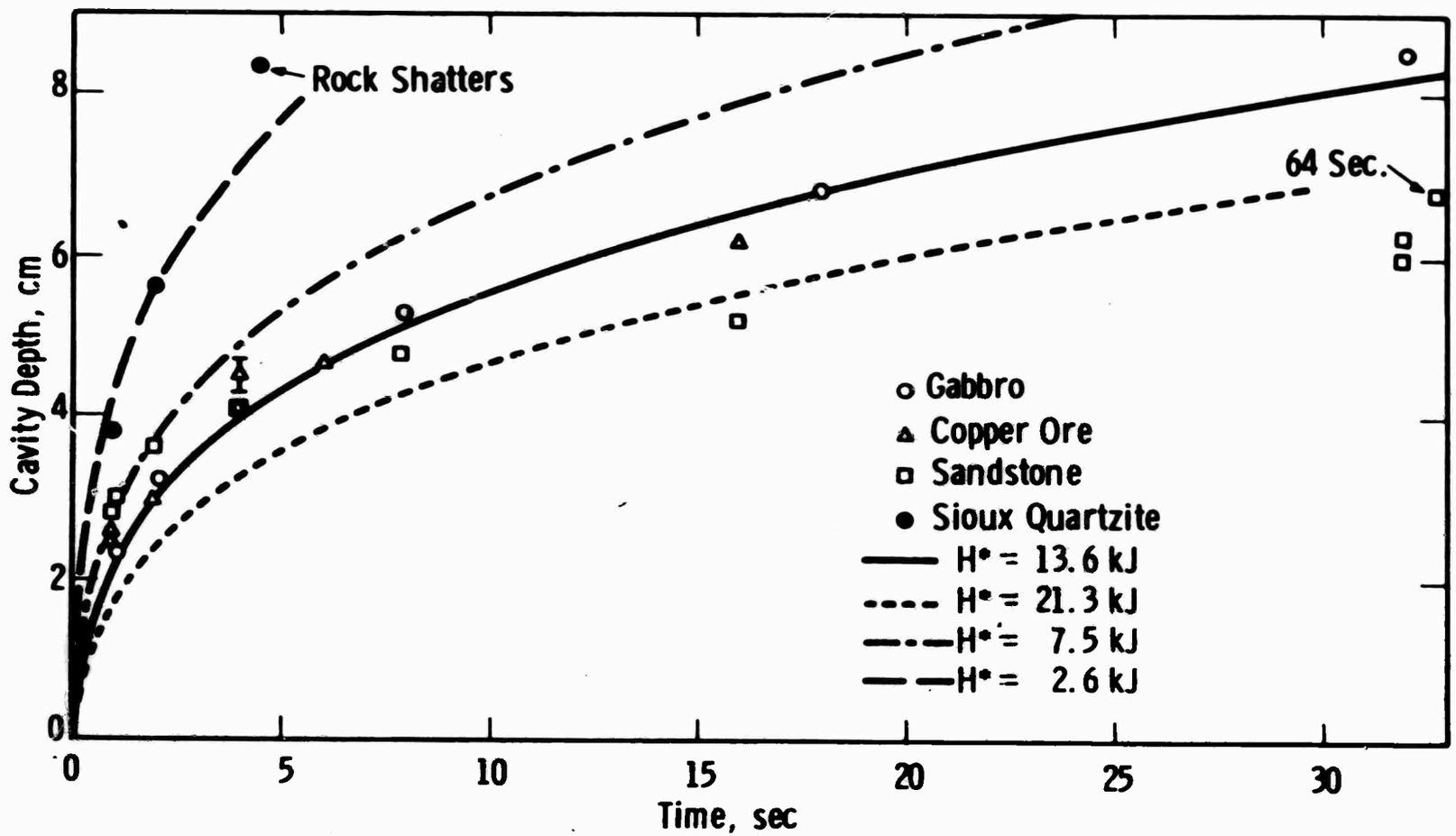

Figure 5-3. Observed and Computed Cavity Growth Rates for Different Rocks and Heats of Removal, H* (Beams Power = 9 kW, 150 k V, Stand-Off Distance = 1/2 inch)

the rock, in copper ore, in a calcareous sandstone, in so-called Sioux quartzite, and in the Oklahoma gabbro. If anything may be concluded from these few tests, then we can say that the initial penetration is perhaps faster than predicted by the theory based on heat of evaporation of $H^* = 14$ kJ. Especially for the sandstone, the later penetration is not as deep as predicted. In quartzite, the cavity is not produced by melting but rather by spallation and the explosive expulsion of small particles; in other words; less energy H^* is needed than for vaporization. The experimental points fall roughly on a curve computed with a value of $H^* = 2.6$ kJ. In this case, the whole experiment was also self-terminating after five seconds when the small block burst into pieces.

Figure 5-3 also shows theoretical curves computed for $H^* = 2.6$ kJ, 7.5 kJ, 13.6 kJ, and 21.3 kJ. The different behavior of the sandstone can perhaps be explained on the basis that, initially, it spalls ($H^* = 7.5$ kJ) and later spalling is inhibited by a layer of molten rock. Alternatively, liquid that keeps flowing into the beam region may inhibit cavity growth. It could also be that heat conduction is greater in the sandstone than in the other rocks and the assumption of an adiabatic process is no longer true.

Obviously, there are many details yet to be investigated but, in general, we feel that our simple theory represents very well the initial piercing rates at least for the first 30 seconds, and it can be used as a basis for the temperature and stress computations.

Another test seemed of interest, namely, to determine the penetration efficiency as a function of beam power. Figure 5-4 shows how cavity depth increases with beam power when the total energy input is held constant. The more quickly a given amount of energy is delivered, the deeper is the cavity, since the adiabatic conditions are more closely approached. When adiabatic conditions are fully obtained, then the cavity depth should no longer depend on beam power. For the gabbro and the 9 kW beam, this is not yet quite the case. Hence, with the higher beam power

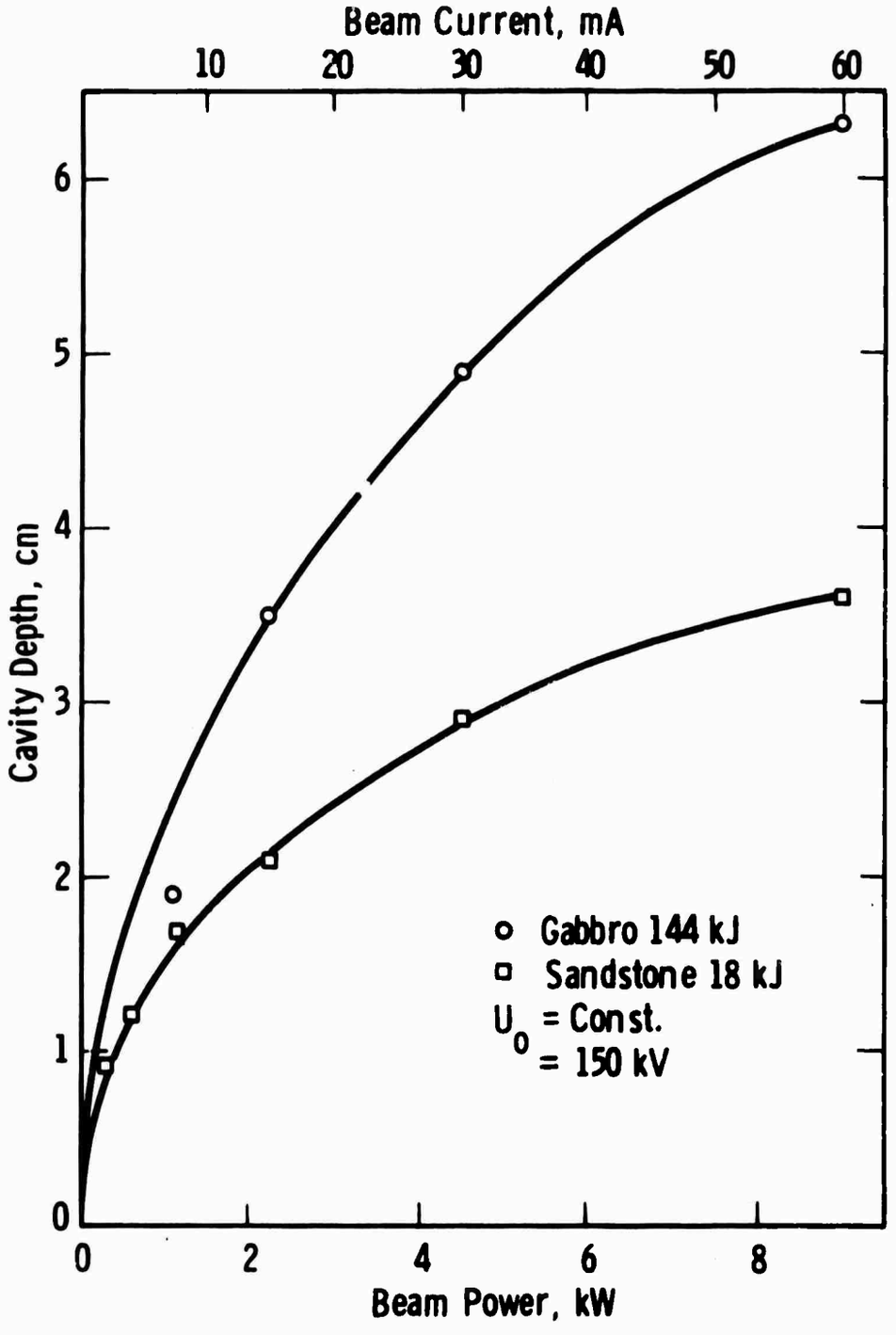

Figure 5-4. Influence of Beam Power on Achieved Piercing Depth for Constant Energy Input

that we will have for the field tests, the piercing rate should increase faster than proportionally with power. Figure 5-4 illustrates rather drastically the importance of the adiabatic conditions and, therefore, the fact that with a low power beam, say 2 kW, one simply can not get representative experiments that provide a valid basis for extrapolation to higher power levels.

As mentioned earlier, the beam width is not entirely determined by beam scattering but also by beam optics, mainly the angular aperture of the beam as it is focused by the magnetic lens. The angular aperture as well as the position of the so-called crossover can be moved by changing the current through the lens. As discussed in Reference 9, the product of angular aperture α_o and diameter of the beam at the focus spot, $\bar{d}_o$, is constant or, in other words, the so-called radiance of the beam is an invariant. If we reduce the angular aperture, we will automatically increase the diameter of the beam at the focus and reduce the power density N*. As to which factor is of the greater importance if we aim for maximum penetration, it depends on the circumstances. For instance, if the power density is already so high that adiabatic conditions prevail, then it is not necessary to increase it further. With our present machine, we can vary the position of the crossover only within narrow limits. But to see whether the focus position is of any importance under our present conditions we made the comparative test with the results listed in Table 5-1. A reduced focus current means the crossover is further away from the orifice of the gun and closer to the top surface of the rock. A small change in focus position will produce an increase in the depth of the cavity of 10 percent in the case of the sandstone and of 17 percent, for the gabbro.

A spinning disc beam analyzer was used to measure beam power profiles. Figure 5-5 shows an example corresponding closely to the conditions of Table 5-1. Total beam current was 60 mA and 150 kV and the plane of measurement, 1/2 inch below the gun exit orifice. At 1.28 A focus current,

Focus Current 1.28 A

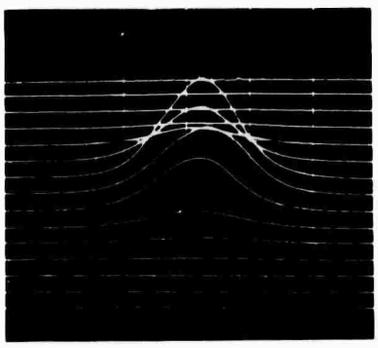

Focus Current 1.14 A

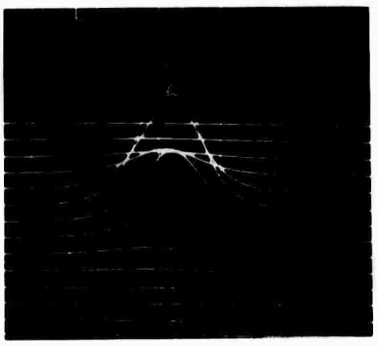

Figure 5-5. Measured Beam Power Density as a Function of Focus Current

optimum beam transmission efficiency was obtained, but at 1.14 A, the beam spot in the plane of measurement is noticeably narrower. The beam angle is also smaller because of the longer focusing distance. The gun was adjusted to keep the beam current the same for both cases. Each trace in Figure 5-5 represents a scan through the beam at various distances from the center axis. The horizontal scale is 1 major division = 0.085 cm; scan lines are separated by 0.04 cm. The vertical scale is arbitrary. Detailed evaluations have not been made at this time.

Our field test gun will have a greater latitude in the position of the beam focus that was available for the test of Table 5-1.

Table 5-1

INFLUENCE OF FOCUS POSITION ON THE DEPTH OF PENETRATION

Rock	Beam Current	Elapsed Time	Focus Current	Cavity Depth	Increase in Cavity Depth
Sandstone	15 mA	8.0 sec	1.30A	2.1 cm	-
"	15	8.0	1.18	2.3	10%
Gabbro	30	8.0	1.30	2.8	-
"	30	8.0	1.24	3.3	17%

(The extent to which the focus could be changed was limited by certain design parameters of this gun.)

Just to collect all the information that is contained in the above tests, and without any attempt at completeness of the analysis, we have plotted in Figure 5-6 the observed depth vs. beam power (as already shown in Figure 5-4) in logarithmic coordinates. Going to higher beam powers, yet keeping the expended energy constant, clearly has advantages.

Figure 5-7 shows the depth-to-width ratio obtained for constant energy input but with various beam powers; there is a marked difference between

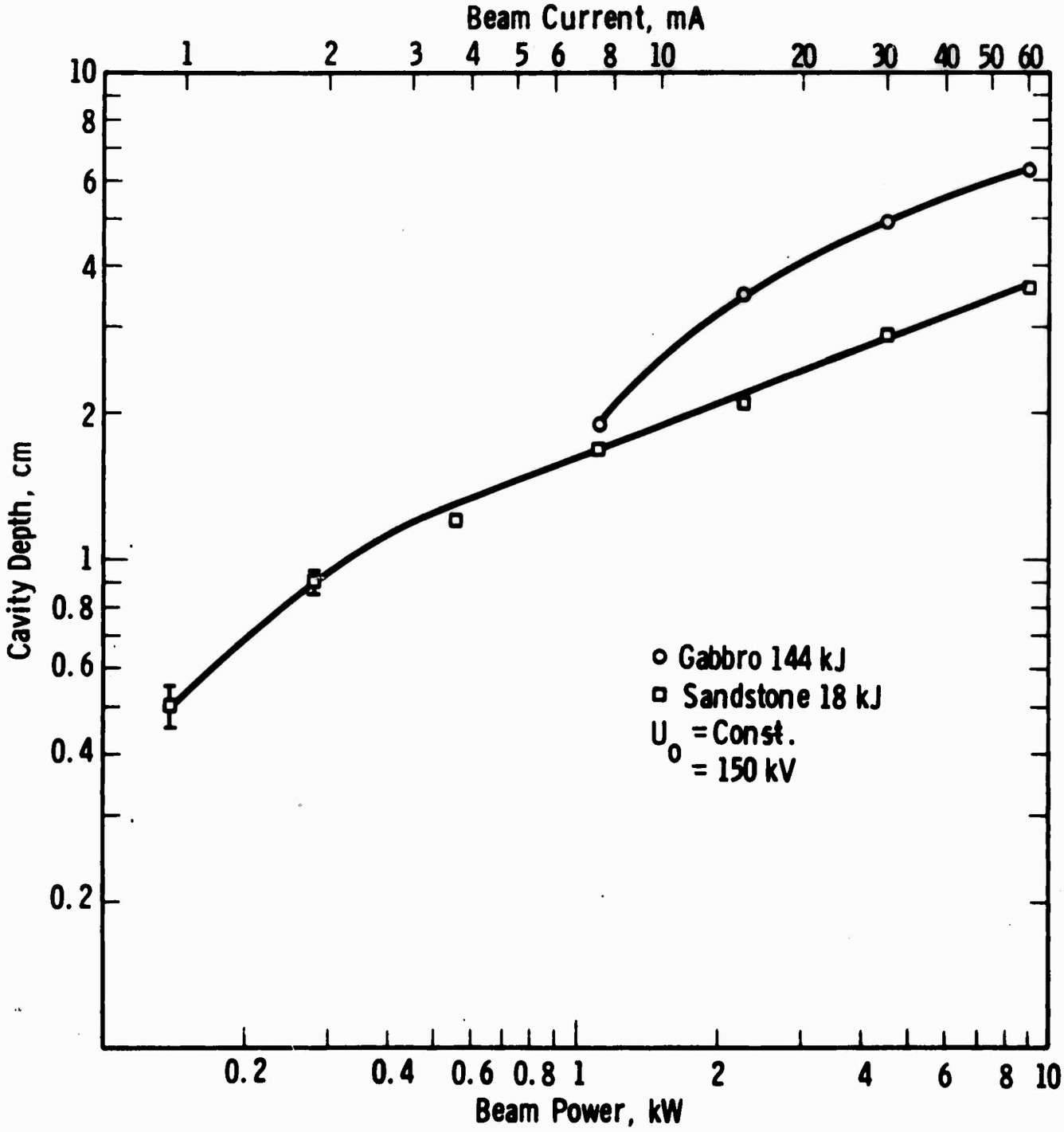

Figure 5-6. Influence of Beam Power on Achieved Piercing Depth for Constant Energy Input (Log-Log Scales)

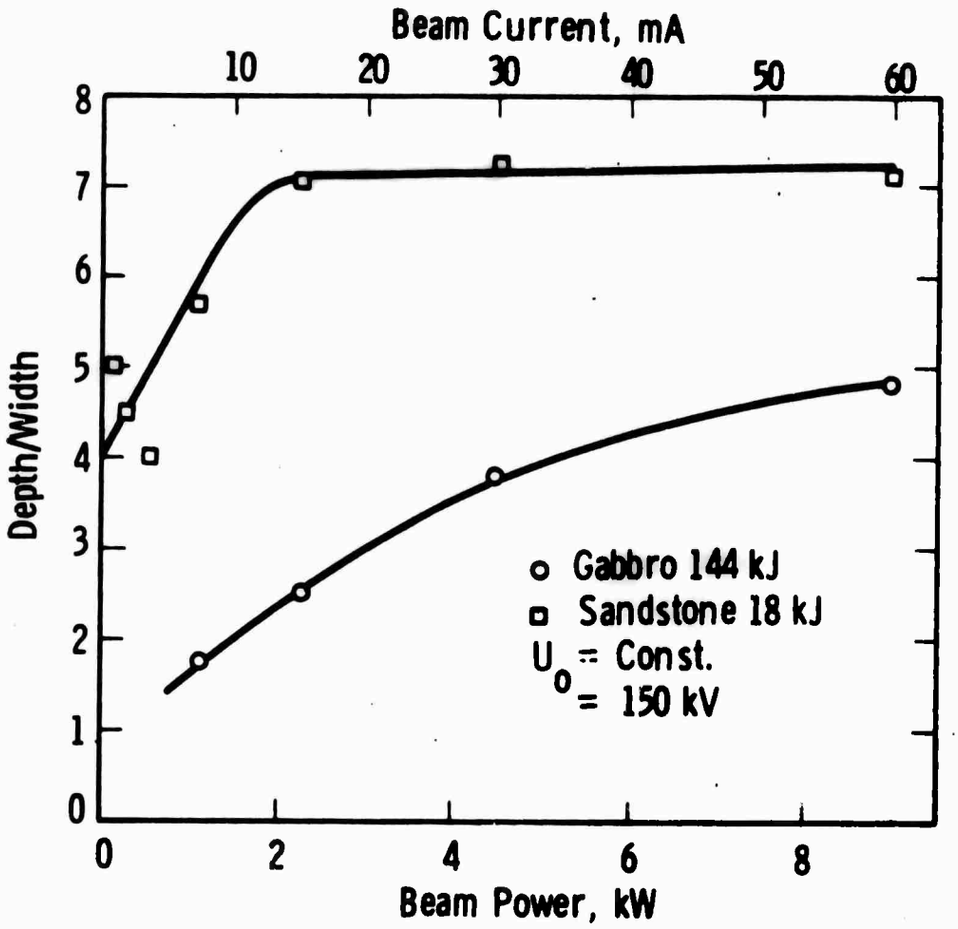

Figure 5-7. Depth/Width Ratios vs Beam Power for Constant Energy Input (Stand-off Distance = 1/2 inch)

sandstone and gabbro. If, however, we plot depth-to-width as a function of depth for a power of 9 kW, as in Figure 5-8, we get initially (for small depths in the order of 1 inch) large differences for different rocks. Yet these disappear when we reach 2 to 4 inches depth. There, the depth-to-width ratio approaches a common value of about 4.25. Because of the limited number of observations, we do not want to speculate on the reasons for this behavior.

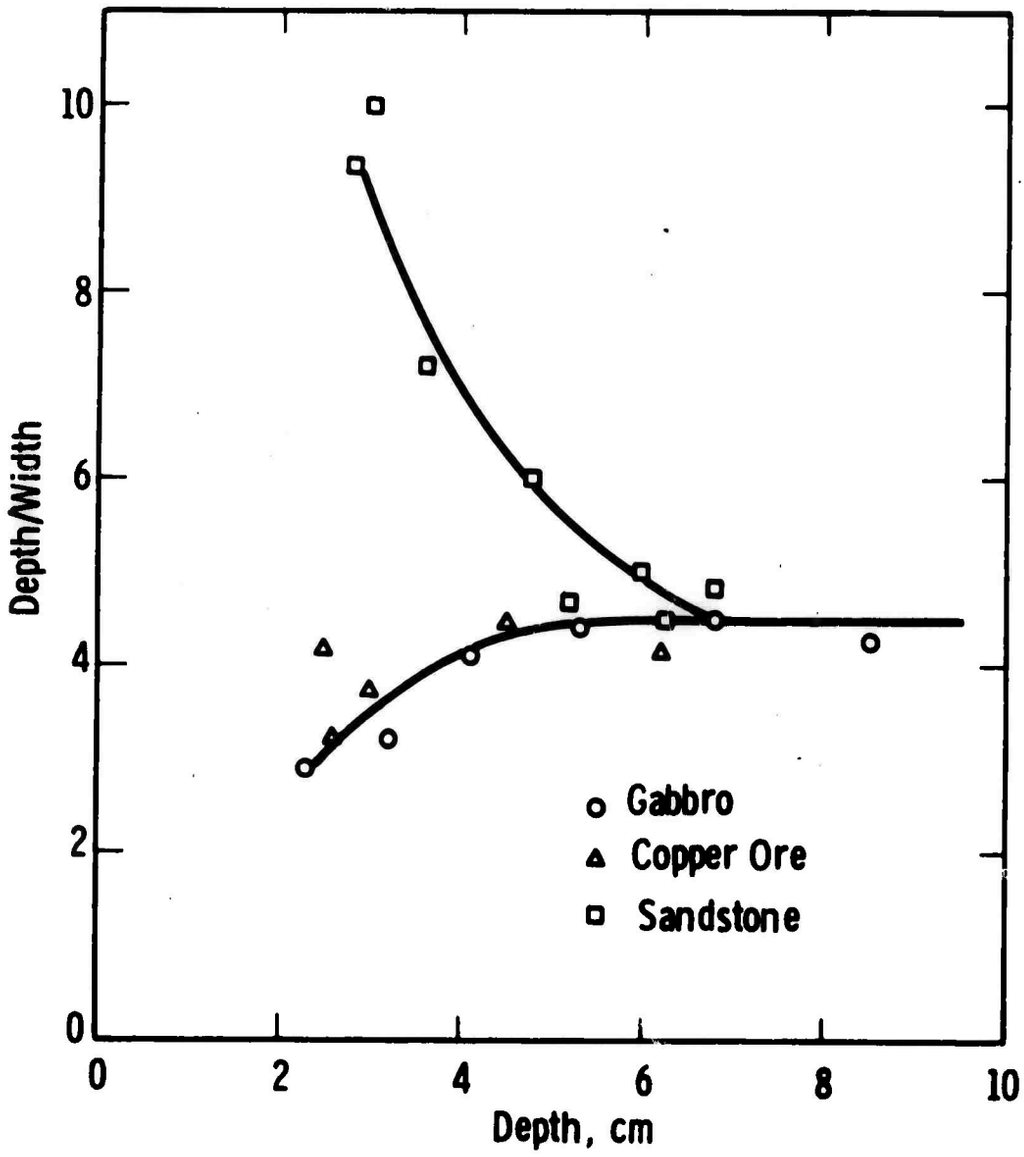

Figure 5-8. Depth (Width Ratio as a Function of Final Depth (Beam Power = 9kW, 150 kV; Stand-off Distance = 1/2 inch)

5.2 OTHER LABORATORY TESTS

Over the past year, we have accumulated a great number of specimens of different types of rock to be used to investigate the efficiency of the electron beam method. However, these tests have been postponed until the higher power machine with horizontal beam is fully operational.

APPENDIX A

CARRIAGE DESIGN SPECIFICATION AND ASSEMBLY DRAWINGS FOR

ELECTRON BEAM GUN

EVALUATION PROGRAM

WESTINGHOUSE ELECTRIC CORPORATION
SUNNYVALE, CALIFORNIA

S-71-1

ELECTRON BEAM GUN
EVALUATION PROGRAM

CARRIAGE DESIGN
SPECIFICATION

No Revision

February 1971

Sponsored By
Advanced Research Projects Agency
ARPA Order Number: 1578
Program Code Number: 0F10

Monitored By Bureau of Mines
Under Contract Number: H0110377
Effective Date of Contract: 11 Dec. 1970
Amount of Contract: $240,000

Prepared By
Senior Engineer
Telephone 408/735-2508

Approved

Approved

ELECTRON BEAM GUN
CARRIAGE DESIGN
SPECIFICATION

CONTENTS

LIST OF FIGURES

ELECTRON BEAM GUN
CARRIAGE DESIGN SPECIFICATION

1.0 SCOPE

This document defines the design parameters and characteristics for an electron beam gun carriage for use in a field test of the gun's rock cutting capabilities.

2.0 INTRODUCTION

2.1 Field Test Program

The field test program is intended to evaluate the electron beam gun as a prime mechanism of fragmentation in a rock excavation process. The test will be conducted in a hard rock field environment with objectives of establishing a correlation between laboratory test data and field results, and determining effects of variables such as standoff distance and cutting speed. A secondary objective of the field tests is to evaluate gun handling and support systems in the field environment.

2.2 Carriage Functions

The carriage and associated equipment are intended for use with the electron beam gun in the field test program. The carriage is the device which supports, manipulates and positions the gun during transport and cutting operations. The carriage also carries ancillary equipment such as vacuum systems or shielding required in close proximity during these operations.

3.0 GENERAL REQUIREMENTS

3.1 Field Test Site

3.1.1 Work Face

The field tests will be conducted on a large, relatively unfractured rock mass. The maximum size of the rock face to be worked from a single carriage location shall be eight feet high by eight feet wide. The base of the six foot square work face shall be at ground level, i.e., in the plane upon which the carriage rests. In order to permit excavation of a tunnel, the total projected frontal area of the gun and carriage assembly must be contained within the six foot square work face outline described above.

3.1.2 Test Site Environment

The field tests will be conducted in surface excavation (quarry) or an underground excavation site. The ground surface can be expected to be crushed rock or earthfill. The carriage shall be designed to withstand and operate under the following environmental conditions:

a) Ambient temperature: variable from $32^{\circ}F$ to $120^{\circ}F$
b) Exposure to direct sunlight
c) Exposure to intermittent rainfall
d) Atmosphere containing abrasive dust or fine rock debris product in excavation process.

3.2 Portability

3.2.1 Site to Site Movement

The carriage shall be designed in such a manner as to facilitate transportation from one work site to another. The carriage may be trailer-mounted or mounted on a skid requiring transportation by truck. In either case the capabilities of a commercial carrier should not be exceeded.

3.2.2 On Site Mobility

The carriage shall have the capability of being moved from one work location to another at the same test site. To achieve this mobility the carriage may be mounted on wheels or equipped with skids for handling with a fork lift. When on location on a work face, the carriage shall be stabilized to prevent carriage movement during cutting operations.

3.2.3 Support System Hook-up

Carriage support systems such as electro-mechanical or electro-hydraulic power supplies, hydraulic reservoirs, etc. shall be designed with portability in mind to minimize field assembly problems.

3.2.4 On Site Assembly

The carriage may be disassembled for transportation from one work site to another, but on-site assembly labor required shall be kept at a minimum. No special tooling or equipment beyond that intended for use in the field test program shall be required. The carriage may require a small crane or light hoisting capability for field assembly.

3.3 Radiation

The electron beam gun produces non-residual X-ray radiation during its operation. Components and materials used in the carriage drive system should be selected with operation and X-ray field as a consideration, or shielded components may be used. Work site shielding and control station shielding is required as outlined in para. 7.1.

4.0 GUN/CARRIAGE/ANCILLARY EQUIPMENT INTERFACES

4.1 Electron Beam Gun Systems

A schematic diagram of the electron beam gun system with ancillary equipment appears in figure 1. Portions of the system mounted on the carriage are indicated in the diagram.

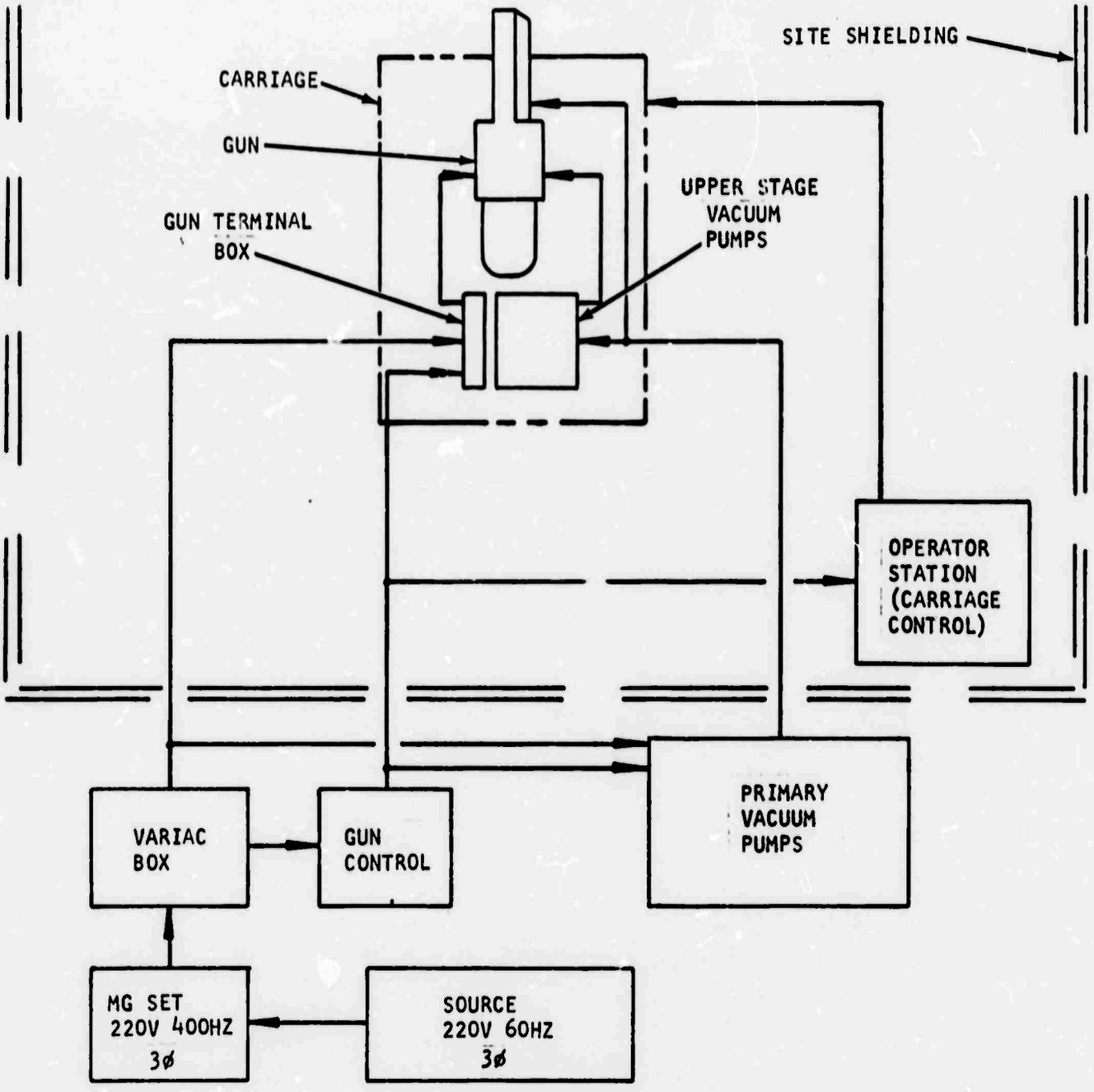

ELECTRON BEAM GUN
SYSTEM SCHEMATIC
FIG. 1.

4.2 Gun/Carriage Interface

4.2.1 EBG Space Envelope

The space envelope required by the electron beam gun is approximated by a rectangular solid 9 feet long by 4-1/2 feet high by 4 feet wide. The EBG electrical terminal box occupies a space 30 inches long by 32 inches high by 9 inches wide. The gun space envelope is shown in figure 2.

4.2.2 Gun Mounts

The mounting or attachment structure of the electron beam gun consists of two structural plates welded to each side of the power supply box in the location shown in figure 2. Each plate has ten drilled and tapped mounting holes as detailed in figure 3.

4.2.3 Weight

The weight of the electron beam gun assembly is approximately 1500 lbs.

4.3 Ancillary Equipment

4.3.1 Space Envelope

The space envelope required for the vacuum pump system for the upper pumping stages is a rectangular solid approximately 32 inches high by 29 inches long by 27 inches wide. This space envelope is illustrated in figure 4. Due to the vacuum system pump capability, the maximum allowable length of the flexible hose connecting the gun and the vacuum system is 6 feet, therefore the upper stage vacuum pump system must be located on or adjacent to the carriage.

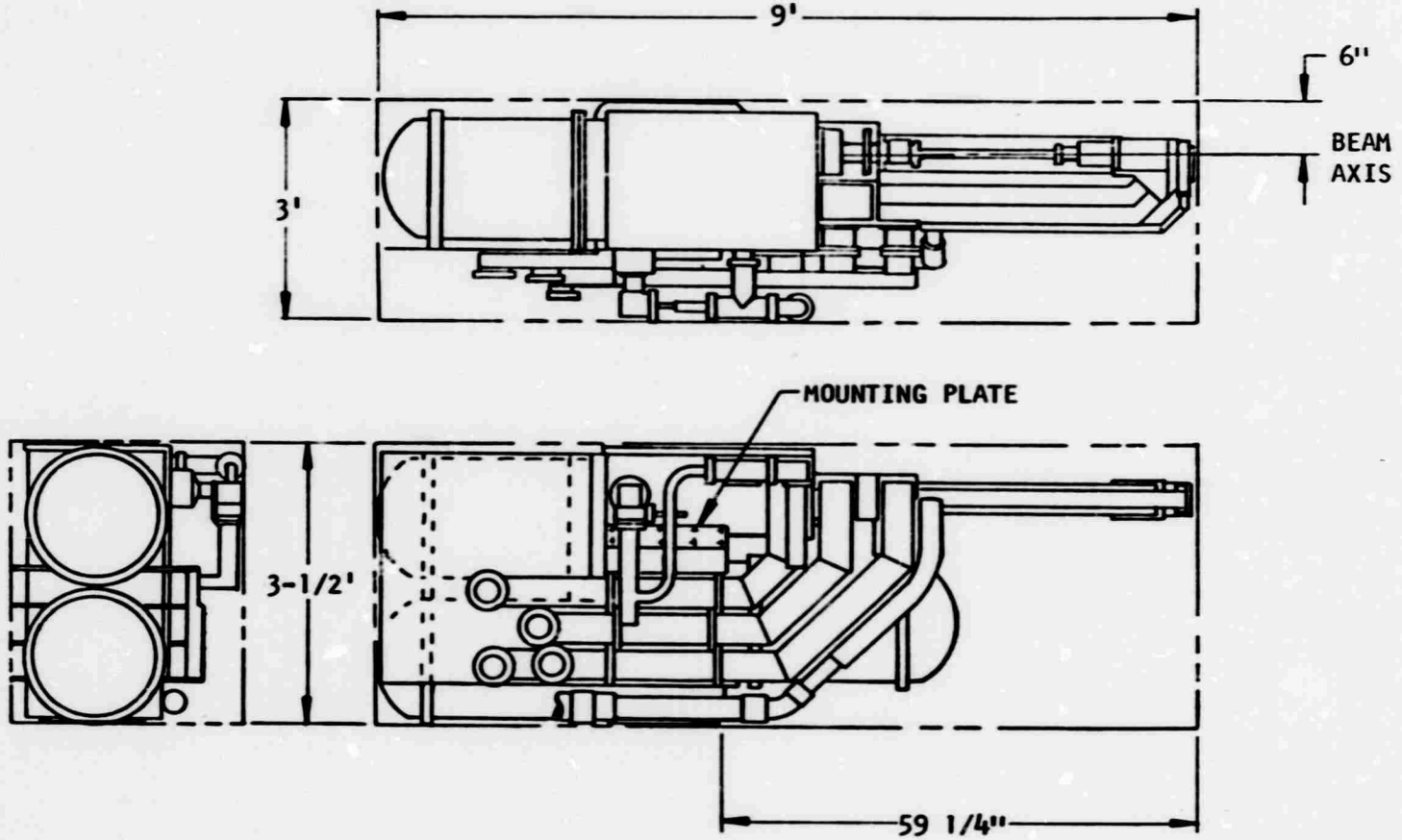

ELECTRON BEAM GUN
SPACE ENVELOPE
FIG. 2

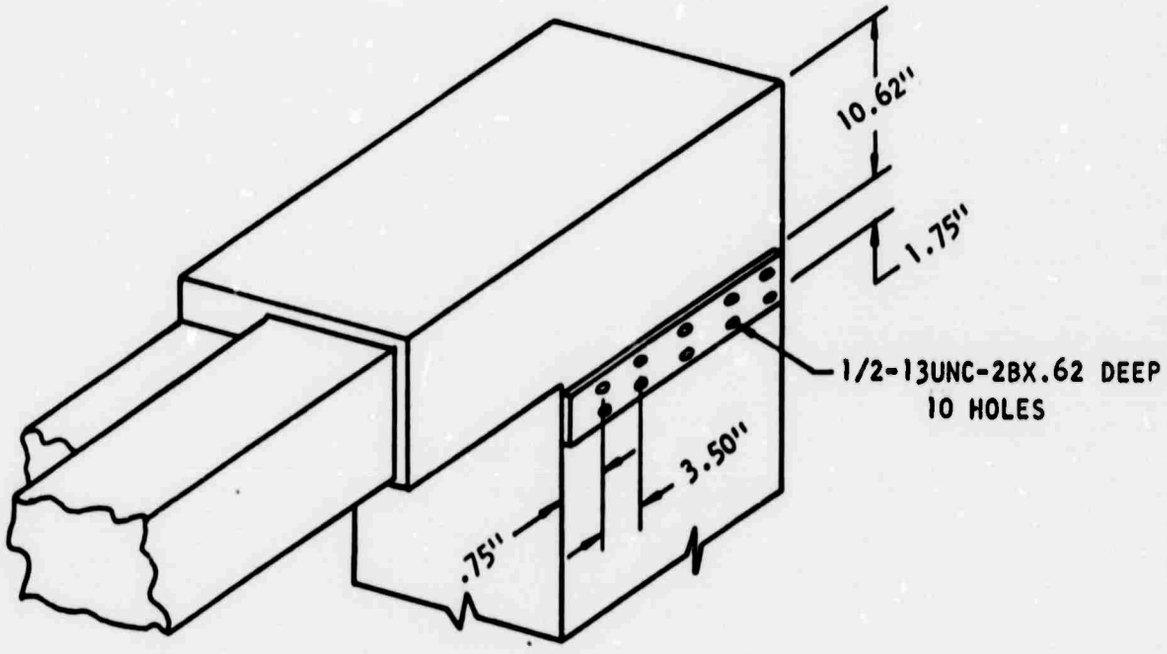

ELECTRON BEAM GUN
MOUNTING DETAILS
(LEFT SIDE SHOWN, RIGHT SIDE
SIMILAR TO OPPOSITE HAND)

FIG. 3

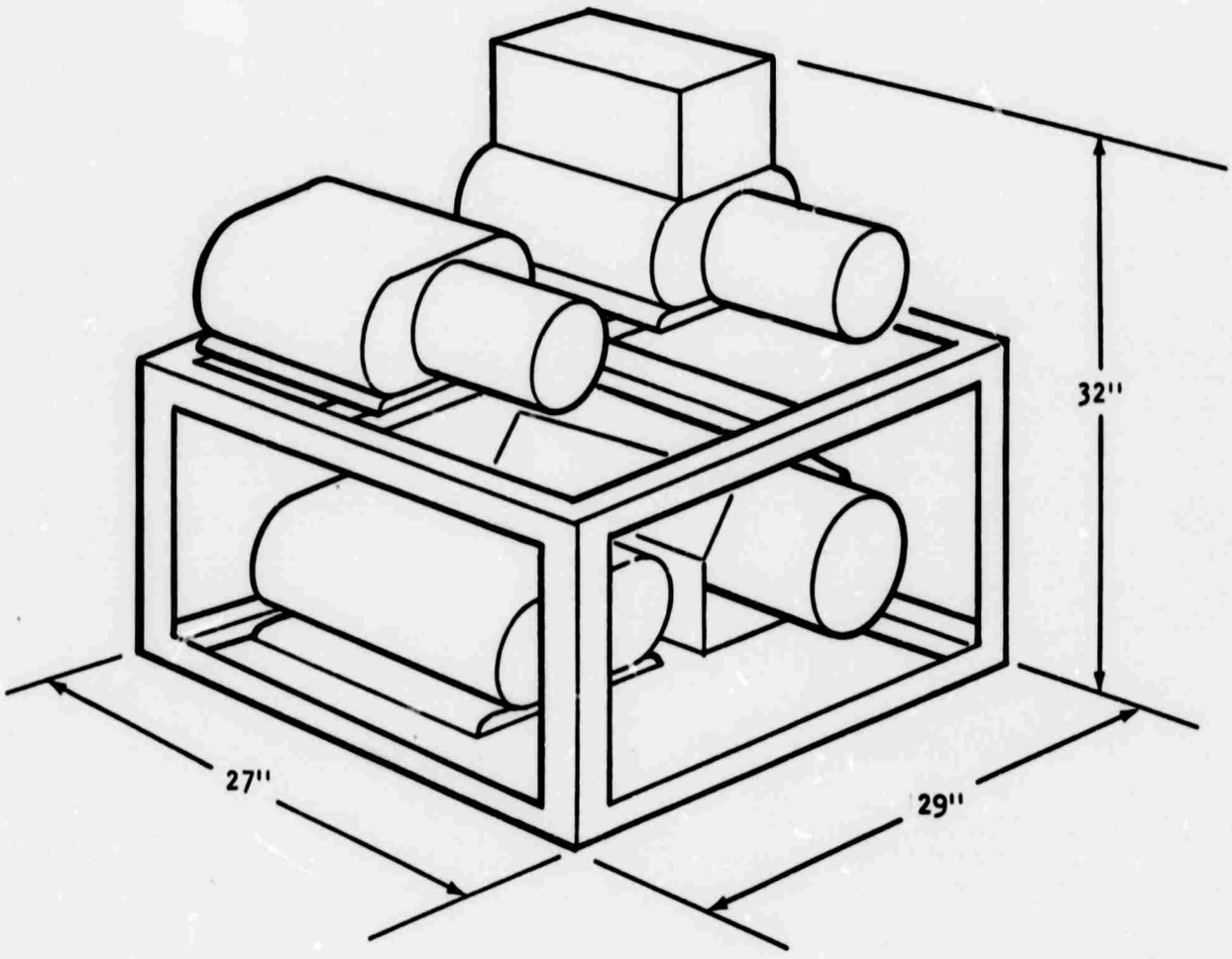

Upper Stage Vacuum Pump System Space Envelope

Figure 4

4.3.2 Vacuum System Mounting

The vacuum system for the upper stages is mounted in a steel frame structure which may be bolted to the carriage or may be mounted on its own dolly within 6 feet of the gun.

4.3.3 Weight

The weight of uperstage vacuum pump system and its steel frame is approximately 675 lbs.

5.0 CARRIAGE PERFORMANCE

5.1 Gun Manipulation

5.1.1 Axis Orientation

For the purpose of describing gun motions the axes shown in figure 5 will be used. The X and Y axes define a vertical plane parallel to the rock face. The Z axis is perpendicular to the X-Y plane and the rock face and coincides with gun center line when the gun is centered on the carriage.

5.1.2 Gun Motions and Limitations

The amount of gun motion may be limited by the distance from the upper stage vacuum pump system as described in para. 4.3. Maximum hose length between this system and the gun is 6 feet. Another limitation is imposed by the oil diffusion pumping system used by the gun. The pumps used must be mounted so that their longitudinal axis does not deviate more than 15^{o} from true vertical.

5.1.2.1 Rotation and Tilt

Rotation and tilt capabilities of the carriage shall be defined in terms of roll, pitch and yaw. Roll refers to rotation of about the Z axis and shall be limited to within 15^{o} of the vertical. Pitch is defined as rotation about

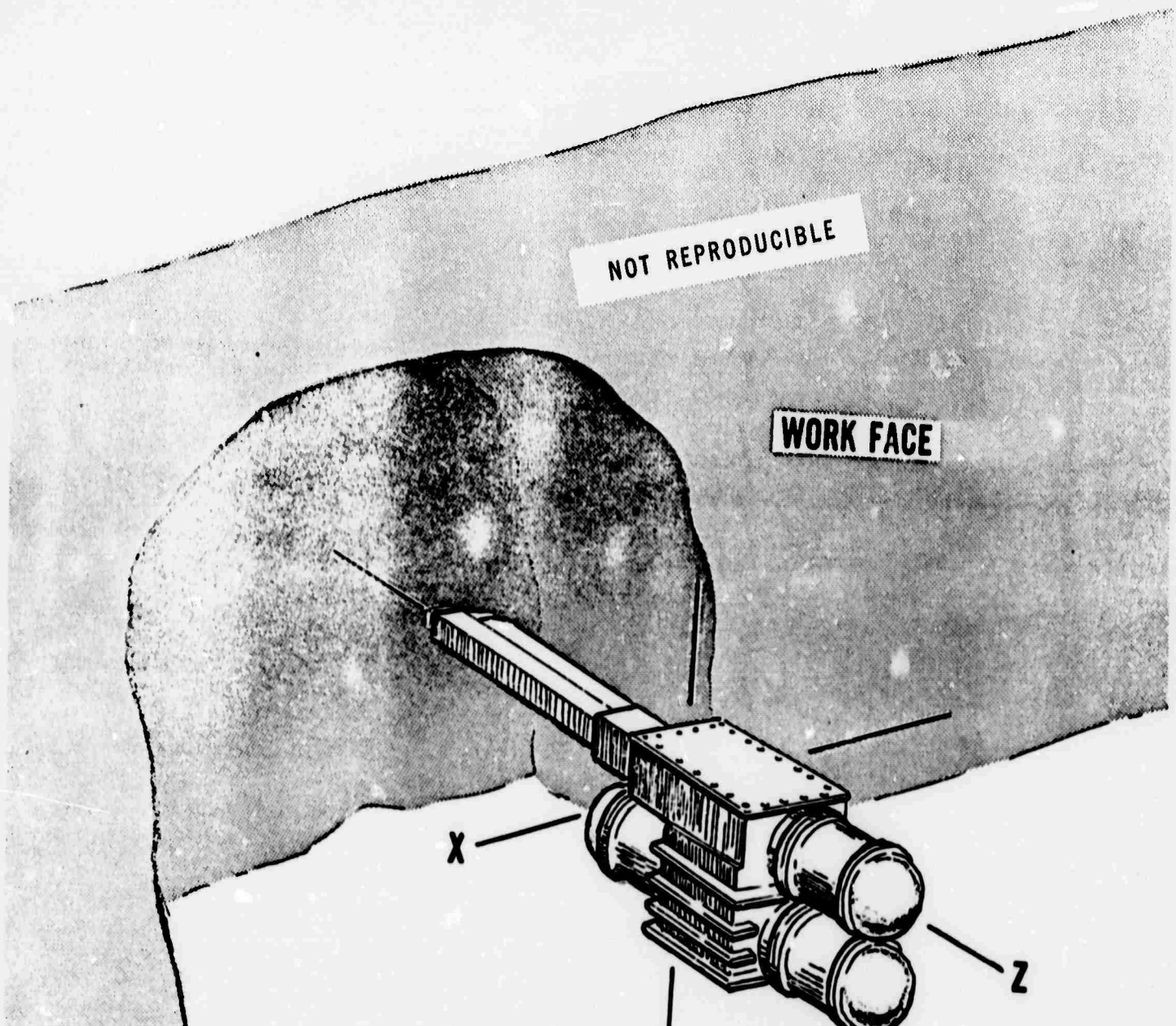

AXIS ORIENTATION
FIG. 5

5.1.2.1 Rotation and Tilt (cont'd)

the X axis, i.e., in the plane defined by the gun transfer column and the vertical, and the gun is limited to a maximum of $\pm$ 15° pitch. The carriage should, however, be designed with the capability for a total pitch angle of 90° such as from 15° above the horizontal axis to 75° below the horizontal axis to enable the gun to reach a work location at the excavation floor. Yaw is defined as rotation in a horizontal plane about the vertical or Y axis there are no limitations on the amount of yaw which can be tolerated. Design yaw capability shall be 45° minimum to either side of the line perpendicular to the work face.

5.1.2.2 X Axis Motion

X axis motion (horizontal traverse) shall be provided as required to enable the gun to work a 6 foot wide face. X-axis motion may be combined with yaw, (rotation about the Y axis,) to achieve the desired width. A minimum of 3 feet of horizontal traverse capability of X axis motion is desirable.

5.1.2.3 Y Axis Motion

Y axis motion (vertical traverse) shall be provided as required to enable the gun to work a 6 foot high rock face. Rotation about the X axis (pitch), may be combined with Y axis motion to achieve the desired work face height.

5.1.2.4 Z Axis Motion

Z axis motion shall be provided to permit some fore and aft movement of gun. The carriage shall be capable of Z axis motion regardless of gun attitude. A minimum of ± 6 inches motion from the nominal gun operating position is required.

5.1.2.5 Velocity of Motions

Motions in Z axis direction may be constant and shall not exceed 15 inches per minute. Velocity in all other modes of operation refers to the velocity of the gun exit nozzle relative to the work face. Velocities during cutting operations shall be variable from 1 inch per minute to 30 inches per minute and shall be controllable to within ± 10 percent.

5.2 Carriage Power System

The required carriage motions and gun manipulations are to be achieved through the use of electro-mechanical or electro-hydraulic power transmission systems. Any hydraulic fluids used should be fire resistant such as a phosphate-ester fluid. Electronic components used in drive systems must be shielded for use in an X-ray field.

6.0 CONTROLS

6.1 Gun Controls

All control stations shall contain master on-off controls for the electron beam gun. The gun control console shall be remote from the carriage and located up to 200 feet from the electron beam gun.

6.2 Carriage Control

6.2.1 Operator's Station

The operator's station shall be remote from the carriage and shall contain all controls necessary to perform gun manipulations during cutting operations. The station shall contain gun on-off controls, equipment for communication to the other stations, and a radiation level monitor interlocked with the gun.

6.2.2 Position Controls

The carriage and manipulation system shall be equipped with controls and drive systems designed to stop the gun in any attitude, in any of its motions, and hold it in that position.

6.2.3 Interlocks

6.2.3.1 Gun Auxiliary Systems

The control system shall be equipped with interlocks as necessary to prevent operation of the electron beam gun without required gun auxiliary systems such as vacuum, water and air.

6.2.3.2 Over-travel

The carriage drive system shall be equipped with over-travel interlocks or limit systems to prevent two-blocking the drive mechanisms.

6.2.3.3 Interference

Limit switches or other sensors shall be located on the transfer column adjacent to the exit nozzle. These shall be interlocked to prevent driving the gun into the work face in any of the modes of the gun motion.

6.2.3.4 Radiation

Radiation interlocks shall be provided as follows:

a) The radiation level monitor in the operator's station shall be interlocked to stop gun operation in the event that the detected emission rate exceeds 20 milliroentgens per hour.

b) The work site shielding doors shall be interlocked to prevent gun operation with open doors.

7.0 SAFETY REQUIREMENTS

7.1 Radiation

Due to X-ray radiation produced by the gun during its operation shielding must be provided for the operator and other field test observers.

7.1.1 Operator's Station

The operator's station shall consist of a plywood booth sheathed with lead .25 inches thick and equipped with leaded glass windows. The control station (para. 6.2) shall be located within this booth. The control station shall be interlocked in accordance with para. 6.2.3.4(a).

7.1.2 Work Site Shielding

The entire work site shall also be shielded for observers' protection by surrounding it with .25 inch lead sheathed plywood fence or equivalent (e.g. 3 or 4 layers of dense concrete block), also equipped with leaded glass windows. Shielding doors shall be interlocked in accordance with para. 6.2.3.4(b).

7.2 Physical Protection

Physical protection is required to minimize the possibility of damage due to rock falling from the work face or from adjacent strata. Gun protection may be incorporated in the carriage or may be obtained from structure covering the work site.

8.0 UTILITIES

The following utilities are required for operation of the electron beam gun.

8.1 Electrical

a) 220 volt, 3 phase, 60 cycle electrical power at 30 KW continuous, 60 KW peak.

b) 220 volt, 3 phase, 400 cycle electrical power 60 KW and 75 KVA.

8.2 Air, Water & Helium

a) Air at 60 lb. per sq. inch and 200 standard cubic feet per minute (20 SCFM for gun and 180 for blast jet use).

b) Water at 15 gallons per minute and 50 lb. per sq. inch, (5 GPM for gun and pump cooling water, 10 GPM for blast jet use and rock face debris removal.

c) Helium, at rate of 300 standard cubic feet per hour while beam is on.

BILL OF MATERIAL

SYM	ITEM	DESCRIPTION		GROUP 1	2	3	4	5	6	7	8	9	10
	122	SCREW, CAP, HEX HD - 1/4-20UNC-2A X 3/4 LG	STL CD PL	19									
	123	SCREW, CAP, HEX HD - 5/16-18UNC-2A X 3/4 LG	STL CD PL	16									
	124	SCREW, CAP, HEX HD - 7/16-14UNC-2A X 1 1/4 LG	STL CD PL	2									
	125	SCREW, CAP, HEX HD - 1/2-13UNC-2A X 1 1/4 LG	STL CD PL	16									
	126	SCREW, CAP, HEX HD - 1/2-13UNC-2A X 1 3/4 LG	STL CD PL	8									
	127	SCREW, CAP, HEX HD - 3/8-16UNC-2A X 3/4 LG	STL CD PL	2									
	128	SCREW, CAP, HEX HD - 1/2-13UNC-2A X 1 1/2 LG	STL CD PL	18									
	129	SCREW, CAP, HEX HD - 3/8-16UNC-2A X 1 IN. LG	STL CD PL	20									
	130	SCREW, CAP, HEX HD - 1/2-13UNC-2A X 1 IN. LG	STL CD PL	36									
	131	SCREW, MACH FL HD - 1/4-20UNC-2A X 5/8 LG	STL CD PL	3									
	132	SCREW, CAP, SKT HD - 3/4-10UNC-3A X 1 1/2 LG	STL CD PL	4									
	133	SCREW, CAP, SKT HD - 3/4-10UNC-3A X 2 IN. LG	STL CD PL	8									
	134	SCREW, CAP, HEX HD - 3/4-10UNC-2A X 1 3/4 LG	STL CD PL	16									
	135	NUT, PLAIN HEX (JAM) - 3/8-16UNC-2B	STL CD PL	26									
	136	NUT, PLAIN HEX - 1/2-13UNC-2B	STL CD PL	8									
	137	NUT, PLAIN HEX - 3/8-16UNC-2B	STL CD PL	2									
	138	WASHER, LOCK SPLIT - #10 NOM	STL CD PL	17									
	139	WASHER, LOCK SPLIT - 1/4 NOM	STL CD PL	27									
	140	WASHER, LOCK SPLIT - 3/8 NOM	STL CD PL	22									
	141	WASHER, LOCK SPLIT - 7/16 NOM	STL CD PL	2									
	142	WASHER, LOCK SPLIT - 1/2 NOM	STL CD PL	72									
	143	WASHER, LOCK SPLIT - 3/4 NOM	STL CD PL	16									
	144	WASHER, LOCK SPLIT - 5/16 NOM	STL CD PL	16									
	145	WASHER, FLAT - 1/4 NOM	STL CD PL	4									
	146	WASHER, FLAT - 1 IN. NOM	STL CD PL	2									
	147	WASHER, FLAT - 1 1/2 NOM	STL CD PL	8									
	148	PIN, COTTER - 1/4 DIA X 2 1/2 LG	STL CD PL	4									
	149	PIN, COTTER - 1/8 DIA X 2 LG	STL CD PL	2									
	150	PIN, SPRING - 1/8 D... 1 1/8 LG	STL CD PL	2									
	151	PIN, SPRING - 1/8 DIA X 1 1/2 LG	STL CD PL	2									
	152	PIN, SPRING - 1/4 DIA X 1 1/2 LG	STL CD PL	4									
4	153	COLLAR - 5/8 SHAFT DIA	BOSTON NO. SC62	2									
H	154	BEARING, FLANGED (OIL IMP) 5/8 I.D. X 7/8 O.D. X 1 IN. LG BRZ	BOSTON NO. FB 1014-8	2									
	155	PIN, SPRING - 1/2 DIA X 1 IN. LG	STL CD PL	4									
	156	SETSCREW, CUP POINT - 1/2-13UNC-2B X 1/2 LG	STL CD PL	2									
	157	WASHER, FLAT - 1/2 NOM	STL CD PL	6									
	158	PIN, SPRING - 1/4 DIA X 3/4 LG	STL CD PL	2									

BILL OF MATERIAL

SYM	ITEM	DESCRIPTION		GROUP 1	2	3	4	5	6	7	8	9	10
	62	ADAPTER	944 J 689-50	6									
	63	SHIM	944 J 689-51	6									
	64	KEY, SQUARE 1/2 X 2 IN. LG	STL	1									
	65	KEY, SQUARE 3/8 X 8 IN. LG	STL	1									
	66	KEY, SQUARE 1/2 X 1 1/2 LG	STL	2									
	67	KEY, SQUARE 1/2 X 1 IN. LG	STL	2									
	68	KEY, SQUARE 1/2 X 2 1/4 LG	STL	1									
	69	KEY, SQUARE 1/4 X 2 1/2 LG	STL	1									
	70	SHIM	944 J 689-52	2									
A	71	HYDRAULIC CYLINDER - UNIVERSAL MODEL NO. MPU3-L, 2 IN. BORE, 18 IN. STROKE, 1 IN. DIA ROD WITH STD MALE STYLE 2 ROD END. NO CUSHIONS		1									
A	72	HYDRAULIC CYLINDER - UNIVERSAL MODEL NO. MPU3-L, 1 1/2 IN. BORE, 26 IN. STROKE, 1 IN. ROD DIA WITH STD MALE STYLE 2 ROD END. CUSHIONED CAP END ONLY.		2									
A	73	HYDRAULIC CYLINDER - UNIVERSAL MODEL NO. MPU3-L, 2 IN. BORE, 30 IN. STROKE, 1 IN. DIA ROD WITH STD MALE STYLE 2 ROD END. NO CUSHIONS		1									
A	74	FEMALE CLEVIS - 3/4-16	UNIVERSAL NO. N20-403	4									
A	75	PIVOT PIN (3/4 DIA X 2 29/32 LG)	UNIVERSAL NO. N20-404	4									
A	76	CLEVIS BRACKET	UNIVERSAL NO. N15-405	4									
A	77	PIVOT PIN (1/2 DIA X 1 7/8 LG)	UNIVERSAL NO. N15-407	4									
B	78	FLANGED CARTRIDGE BEARING - STD SERIES 1 15/16 DIA	FAFNIR NO. [illegible]16	6									
B	79	FLANGED CARTRIDGE BEARING - STD SERIES 1 1/2 DIA	FAFNIR NO. [illegible] 1/2	1									
C	80	BEARING - ECONO-TRAK SERIES 2000	ROTEK NO. L4-17P1Z	1									
C	81	BEARING - ECONO-TRAK SERIES 1000	ROTEK NO. M-26P4Z	1									
D	82	ROTARY ACTUATOR - 7,500 LB/IN TORQUE 180° 2 RACK SOLID SHAFT	MODEL NO. SH 7,500	1									
D	83	ROTARY ACTUATOR - 30,000 LB/IN TORQUE 360° 2 RACK HOLLOW SHAFT	MODEL NO. HS 30,000										
J	84	WHEEL - 12 IN. DIA X 4 IN. WIDE (4 1/4 HUB WIDTH) 1 1/2 BORE THRU BRG - 4800 LB CAPACITY	ALBION NO. PY-12701	4									
F	85	TROLLEY WHEEL (3 1/8 NOM DIA)	NICE NO. 4955-2	22									
F	86	TROLLEY WHEEL (2 1/8 NOM DIA)	NICE NO. 5646	6									
E	87	SPROCKET - 1/2 PITCH,25 TEETH,TYPE B HUB - STL, BORED TO 1 IN. DIA WITH KEY SEAT & TWO SET SCREWS (KEY SEAT MUST BE IN LINE WITH CENTER OF ONE TOOTH WITHIN .030)	ACME NO. 40825	2									
E	88	SPROCKET - 1/2 PITCH,10 TEETH,TYPE B HUB - STL,STK 1/2 IN. BORE NO SETSCREW	ACME NO. 40810	1									
E	89	SPROCKET - 5/8 PITCH,11 TEETH,TYPE B HUB - STL,STK 5/8 IN. BORE NO SETSCREW	ACME NO. 50811	2									
E	90	SPROCKET - 5/8 PITCH,23 TEETH,TYPE B HUB - STL, BORED TO 2 IN. DIA WITH KEY SEAT & TWO SETSCREWS (KEY SEAT MUST BE IN LINE WITH CENTER OF ONE TOOTH WITHIN .030)	ACME NO. 50823	2									
E	91	SPROCKET - 5/8 PITCH,19 TEETH,TYPE A PLATE STL,STK 5/8 BORE		2									
E	92	SPROCKET - 5/8 PITCH,24 TEETH,TYPE B HUB STL,BORED TO 2 IN. DIA WITH KEY SEAT & TWO SETSCREWS (KEY SEAT MUST BE IN LINE WITH CENTER OF ONE TOOTH WITHIN .030)	ACME NO. 50824	2									
E	93	SPROCKET - 1 1/4 PITCH,11 TEETH,TYPE B HUB STL BORED TO 1 1/2 DIA WITH KEYSEAT & TWO SETSCREWS	ACME NO. 100811	1									
E	94	SPROCKET - 1 1/4 PITCH,32 TEETH,TYPE B HUB STL BORED TO 2 IN. DIA WITH KEY SEAT & TWO SETSCREWS	ACME NO. 100832	1									
G	96	ROLLER CHAIN - 1/2 PITCH ASA NO. 40 SINGLE WIDTH X 239 PITCHES		1									
G	97	ROLLER CHAIN - 1/2 PITCH ASA NO. 40 SINGLE WIDTH X 229 PITCHES		1									
G	98	ROLLER CHAIN - 1/2 PITCH ASA NO. 40 SINGLE WIDTH X 99 PITCHES		1									
G	99	ROLLER CHAIN - 1/2 PITCH ASA NO. 40 SINGLE WIDTH X 369 PITCHES		1									
G	100	ROLLER CHAIN - 5/8 PITCH ASA NO. 50 SINGLE WIDTH X 173 PITCHES		2									
G	101	ROLLER CHAIN - 5/8 PITCH ASA NO. 50 SINGLE WIDTH X 177 PITCHES		2									
G	102	ROLLER CHAIN - 1 1/4 PITCH ASA NO. 100 SINGLE WIDTH,RIVETED, 40 PITCHES		1									
G	103	CONNECTING LINK FOR ASA NO. 40 ROLLER CHAIN		9									
G	104	CONNECTING LINK FOR ASA NO. 50 ROLLER CHAIN		9									
G	105	CONNECTING LINK FOR ASA NO. 100 ROLLER CHAIN		1									
G	106	OFFSET LINK FOR ASA NO. 40 ROLLER CHAIN		4									
G	107	OFFSET LINK FOR ASA NO. 50 ROLLER CHAIN		4									
G	108	OFFSET LINK FOR ASA NO. 100 ROLLER CHAIN		1									
H	109	COLLAR - 2 IN. SHAFT DIA	BOSTON NO. SC200	2									
H	110	BEARING, FLANGED (OIL IMP) 3/8 I.D. X 3/4 O.D. X 3/4 LG BRZ	BOSTON NO. FB-1012-6	4									
H	111	BEARING, FLANGED (OIL IMP) 1/2 I.D. X 5/8 O.D. X 3/4 LG BRZ	BOSTON NO. FB-810-6	6									
H	112	BEARING, FLANGED (OIL IMP) 1/2 I.D. X 5/8 O.D. X 1 IN. LG BRZ	BOSTON NO. FB-810-8	1									
H	113	BEARING, FLANGED (OIL IMP) 1/2 I.D. X 5/8 O.D. X 3 3/4 LG BRZ	BOSTON NO. FB-810-4	1									
H	114	BEARING, FLANGED (OIL IMP) 1 IN. I.D. X 1 1/4 O.D. X 3/4 LG BRZ	BOSTON NO. FB-1620-6	2									
	115	KEY, SQUARE - 3/16 X 3 1/2 LG	STL	1									
	116	SCREW, MACH FL HD - 1/2-13UNC-2A X 2 IN. LG	STL CD PL	22									
	117	SCREW, MACH FL HD - 1/2-13UNC-2A X 1 1/2 LG	STL CD PL	6									
	118	SCREW, MACH PAN HD - #10-24UNC-2A X 1 1/2 LG	STL CD PL	9									
	119	SCREW, CAP, HEX HD - #10-24UNC-2A X 1 1/2 LG	STL CD PL	9									
	120	SCREW, CAP, HEX HD 1/4-20UNC-2B X 1 1/2 LG	STL CD PL	6									
	121	SCREW, CAP, HEX HD - 1/4-20UNC-2B X 5/8 LG	STL CD PL	9									

A-15a

BILL OF MATERIAL

DESCRIPTION		GROUP 1	2	3	4	5	6	7	8	9	10
ADAPTER	944 J 689-50		6								
SHIM	944 J 689-51		6								
KEY, SQUARE 1/2 X 2 IN. LG	STL		1								
KEY, SQUARE 3/8 X 8 IN. LG	STL		1								
KEY, SQUARE 1/2 X 1 1/2 LG	STL		2								
KEY, SQUARE 1/2 X 1 IN. LG	STL		2								
KEY, SQUARE 1/2 X 2 1/4 LG	STL		1								
KEY, SQUARE 1/4 X 2 1/2 LG	STL		1								
SHIM	944 J 689-52		2								
HYDRAULIC CYLINDER - UNIVERSAL MODEL NO. MPU3-L; 2 IN. BORE, 18 IN. STROKE, 1 IN. DIA ROD WITH STD MALE STYLE 2 ROD END, NO CUSHIONS			1								
HYDRAULIC CYLINDER - UNIVERSAL MODEL NO. MPU3-L; 3 1/2 IN. BORE, 26 IN. STROKE, 1 IN. ROD DIA WITH STD MALE STYLE 2 ROD END, CUSHIONED-CAP END ONLY.			2								
HYDRAULIC CYLINDER - UNIVERSAL MODEL NO. MPU3-L; 2 IN. BORE, 30 IN. STROKE, 1 IN. DIA ROD WITH STD MALE STYLE 2 ROD END, NO CUSHIONS			1								
MALE CLEVIS - 3/4-16	UNIVERSAL NO. N20-403		4								
PIVOT PIN (3/4 DIA X 2 29/32 LG)	UNIVERSAL NO. N20-404		4								
CLEVIS BRACKET	UNIVERSAL NO. N15-405		4								
PIVOT PIN (1/2 DIA X 3 7/8 LG)	UNIVERSAL NO. N15-407		4								
ANGLED CARTRIDGE BEARING - STD SERIES 1 15/16 DIA BORE	[illegible] NO. 16		6								
ANGLED CARTRIDGE BEARING - STD SERIES 1 1/2 DIA BORE	[illegible] NO. [illegible]		1								
BEARING - ECONO-TRAK SERIES 2000	ROTEK NO. L4-17P12		1								
BEARING - ECONO-TRAK SERIES 1000	ROTEK NO. M4-26P42		1								
ROTARY ACTUATOR - 7,500 LB/IN TORQUE 180° 2 RACK SOLID SHAFT	MODEL NO. SH 7,500		1								
ROTARY ACTUATOR - 30,000 LB/IN TORQUE 360° 2 RACK HOLLOW SHAFT	MODEL NO. HS 30,000										
GEAR - 32 IN. DIA X 4 IN. WIDE (4 1/4 HUB WIDTH) 1 1/2 BORE THRU BRG - 4800 LB. CAPACITY	ALBION NO. PY-12701		4								
PULLEY WHEEL (3 1/8 NOM DIA)	NICE NO. 4935-2		22								
PULLEY WHEEL (2 1/8 NOM DIA)	NICE NO. 5646		6								
SPROCKET - 1/2 PITCH,25 TEETH,TYPE B HUB - STL, BORED TO 1 IN. DIA WITH KEY SEAT & TWO SET SCREWS (KEY SEAT MUST BE IN LINE WITH CENTER OF ONE TOOTH WITHIN .003)	ACME NO. 40825		2								
SPROCKET - 1/2 PITCH,10 TEETH,TYPE B HUB - STL,STK 1 1/2 IN. BORE NO SETSCREW	ACME NO. 40810		1								
SPROCKET - 5/8 PITCH,11 TEETH,TYPE B HUB - STL,STK 5/8 IN. BORE NO SETSCREW	ACME NO. 50811		2								
SPROCKET - 5/8 PITCH,23 TEETH,TYPE B HUB - STL, BORED TO 2 IN. DIA WITH KEY SEAT & TWO SETSCREWS (KEY SEAT MUST BE IN LINE WITH CENTER OF ONE TOOTH WITHIN .0303)	ACME NO. 50823		2								
SPROCKET - 5/8 PITCH,19 TEETH,TYPE A PLATE STL,STK 5/8 BORE			2								
SPROCKET - 5/8 PITCH,24 TEETH,TYPE B HUB STL,BORED TO 2 IN. DIA WITH KEY SEAT & TWO SETSCREWS (KEY SEAT MUST BE IN LINE WITH CENTER OF ONE TOOTH WITHIN .0303)	ACME NO. 50828		2								
SPROCKET - 1 1/4 PITCH,11 TEETH,TYPE B HUB STL BORED TO 1 1/2 DIA WITH KEYSEAT & TWO SETSCREWS	ACME NO. 100811		1								
SPROCKET - 1 1/4 PITCH,32 TEETH,TYPE B HUB STL BORED TO 2 IN. DIA WITH KEY SEAT & TWO SETSCREWS	ACME NO. 100832		1								
ROLLER CHAIN - 1/2 PITCH ASA NO. 40 SINGLE WIDTH X 239 PITCHES			1								
ROLLER CHAIN - 1/2 PITCH ASA NO. 40 SINGLE WIDTH X 229 PITCHES			1								
ROLLER CHAIN - 1/2 PITCH ASA NO. 40 SINGLE WIDTH X 99 PITCHES			1								
ROLLER CHAIN - 1/2 PITCH ASA NO. 40 SINGLE WIDTH X 86.9 PITCHES			1								
ROLLER CHAIN - 3/8 PITCH ASA NO. 35 SINGLE WIDTH X 177 PITCHES			2								
ROLLER CHAIN - 3/8 PITCH ASA NO. 35 SINGLE WIDTH X 177 PITCHES			2								
ROLLER CHAIN - 1 1/4 PITCH ASA NO. 100 SINGLE WIDTH,RIVETED, 40 PITCHES			1								
CONNECTING LINK FOR ASA NO. 40 ROLLER CHAIN			8								
CONNECTING LINK FOR ASA NO. 50 ROLLER CHAIN			2								
CONNECTING LINK FOR ASA NO. 100 ROLLER CHAIN			1								
OFFSET LINK FOR ASA NO. 40 ROLLER CHAIN			4								
OFFSET LINK FOR ASA NO. 50 ROLLER CHAIN			2								
OFFSET LINK FOR ASA NO. 100 ROLLER CHAIN			1								
COUPLING - 2 IN. SHAFT DIA	BOSTON NO. S6200		2								
FLANGE, FLANGED (OIL IMPT) 5/8 I.D. X 3/4 O.D. X 3/4 LG BRZ.	BOSTON NO. FB-1011-6		4								
FLANGE, FLANGED (OIL IMPT) 1/2 I.D. X 5/8 O.D. X 3/4 LG BRZ	BOSTON NO. FB-810-6		8								
FLANGE, FLANGED (OIL IMPT) 1/2 I.D. X 3/8 O.D. X 1 IN. LG BRZ	BOSTON NO. FB-810-8		1								
FLANGE, FLANGED (OIL IMPT) 1/2 I.D. X 7/8 O.D. X 1 1/4 LG BRZ	BOSTON NO. FB-810-4		1								
FLANGE, FLANGED (OIL IMPT) 1 IN. I.D. X 1 1/4 O.D. X 2 LG BRZ	BOSTON NO. FB-1620-4		2								
KEY - 1/4 X 1 1/2 LG	STL		1								
MACH FL HD - 1/2-13UNC-2A X 2 IN. LG	STL CD PL		22								
MACH FL HD - 1/2-13UNC-2A X 1 1/2 LG	STL CD PL		8								
MACH PAN HD - 5/16-24UNC-2A X 1 1/2 LG	STL CD PL		2								
MACH HEX HD - 5/16-24UNC-2A X 1 1/2 LG	STL CD PL		2								
CAP, HEX HD 1/4-20UNC-2A X 1 1/2 LG	STL CD PL		4								
CAP, HEX HD 1/4-20UNC-2A X 3/4 LG	STL CD PL		8								

BILL OF MATERIAL

SYM	ITEM	DESCRIPTION		GROUP 1	2	3	4	5	6	7	8	9	10
	1	ELECTRON BEAM GUN CARRIAGE	GR 2 THIS DWG	1									
	2	TRAILER FRAME	944 J 689-16		1								
	3	BRACE, TRAILER FRAME	944 J 689-32		1								
	4	CARRIAGE	944 J 689-38		1								
	5	CARRIAGE	944 J 688-4		1								
	6	CARRIAGE	944 J 690-15		1								
	7	BEAM	944 J 688-43		1								
	8	BEAM	944 J 688-44		1								
	9	PIVOT BASE	944 J 688-33		1								
	10	BEARING PLATE	944-J-690-1		1								
	11	BOGIE	944 J 690-4		1								
	12	CARRIAGE	944 J 688-24		1								
	13	CARRIAGE	944 J 688-30		1								
	14	SPROCKET HOUSING	944 J 690-11		1								
	15	FLANGE	944 J 690-19		1								
	16	BRACKET, GUN MOUNTING	944 J 690-51		1								
	17	BRACKET, GUN MOUNTING	944 J 690-52		1								
	18	SHAFT, PITCH	944 J 690-45		1								
	19	SHAFT, TORSION	944 J 690-43		1								
	20	SHAFT, TORSION	944 J 690-44		1								
	21	PIN	944 J 690-56		1								
	22	SPROCKET BRACKET	944 J 690-47		2								
	23	BRACKET	944 J 690-39		1								
	24	ANGLE	944 J 690-42		2								
	25	CHAIN ADJUSTER	944 J 688-49		4								
	26	CHAIN ADJUSTER	944 J 688-50		4								
	27	CHAIN ADJUSTER	944 J 688-51		8								
	28	PIN (1/2 DIA X 3.00)	944 J 688-61		1								
	29	SPROCKET SHAFT	944 J 688-58		2								
	30	PIN	944 J 688-59		4								
	31	MOUNTING PLATE	944 J 688-60		1								
	32	SHAFT, PITCH DRIVE	944 J 690-46		1								
	33	SHAFT	944 J 688-57		1								
	34	PIN (1.7 DIA X 2.62)	944 J 688-53		1								
	35	PIN (1/2 DIA X 3.62)	944 J 688-55		1								
	36	PIN (1.8 DIA X 3.00)	944 J 688-56		2								
	37	WHEEL ADJUSTER	944 J 688-21		1								
	38	BRIDGE	944 J 688-1		1								
	39	BEARING BLOCK	944 J 688-2		1								
	40	BEARING BLOCK	944 J 688-3		1								
	41	SPROCKET SUB-ASSY	944 J 689-1		1								
	42	CHAIN GUIDE	944 J 689-5		1								
	43	CHAIN GUIDE	944 J 689-6		1								
	44	SHIM	944 J 690-55		2								
	45	CHAIN GUIDE	944 J 689-7		2								
	46	CHAIN GUIDE	944 J 689-8		2								
	47	CHAIN GUIDE	944 J 689-9		1								
	48	CHAIN GUIDE	944 J 689-10		1								
	49	CHAIN GUIDE	944 J 689-11		1								
	50	CHAIN GUIDE	944 J 689-12		1								
	51	CHAIN GUIDE	944 J 689-13		1								
	52	CHAIN GUIDE	944 J 689-14		1								
	53	CHAIN GUIDE	944 J 689-15		1								
	54	SPROCKET BRACKET	944 J 690-22		1								
	55	SPROCKET BRACKET	944 J 690-23		1								
	56	SPROCKET BRACKET	944 J 690-24		1								
	57	SPROCKET BRACKET	944 J 690-25		1								
	58	SHIM	944 J 690-9		14								
	59	SHIM	944 J 690-10		6								
	60	CHAIN GUIDE	944 J 689-49		1								
	61	WHEEL BRACKET	944 J 690-42		6								

REVISIONS			
REV	ZONE	DESCRIPTION	APP

A, MAY BE PURCHASED FROM UNIVERSAL FLUID DYNAMICS CO., ALPENA, MICHIGAN.

B, MAY BE PURCHASED FROM FAFNIR

C, MAY BE PURCHASED FROM ROTEK INC., ARVENAL, OHIO

C, MAY BE PURCHASED FROM FID-TORK DIV., ALLEN ELECTRIC & EQUIPMENT CO., DAYTLEE, OHIO.

E, MAY BE PURCHASED FROM ALBION INDUSTRIES INC., ALBION MICHIGAN.

F, MAY BE PURCHASED FROM NICE BALL BEARING CO., PHILADELPHIA, PENN.

G, MAY BE PURCHASED FROM ACME CHAIN CORP., HOLYOKE, MASS. OR EQUAL.

H, MAY BE PURCHASED FROM BOSTON GEAR, QUINCY, MASS.

DO NOT SCALE THIS DWG.

WESTINGHOUSE ELECTRIC CORPORATION

ELECTRON BEAM GUN CARRIAGE ASSY

944J687

B

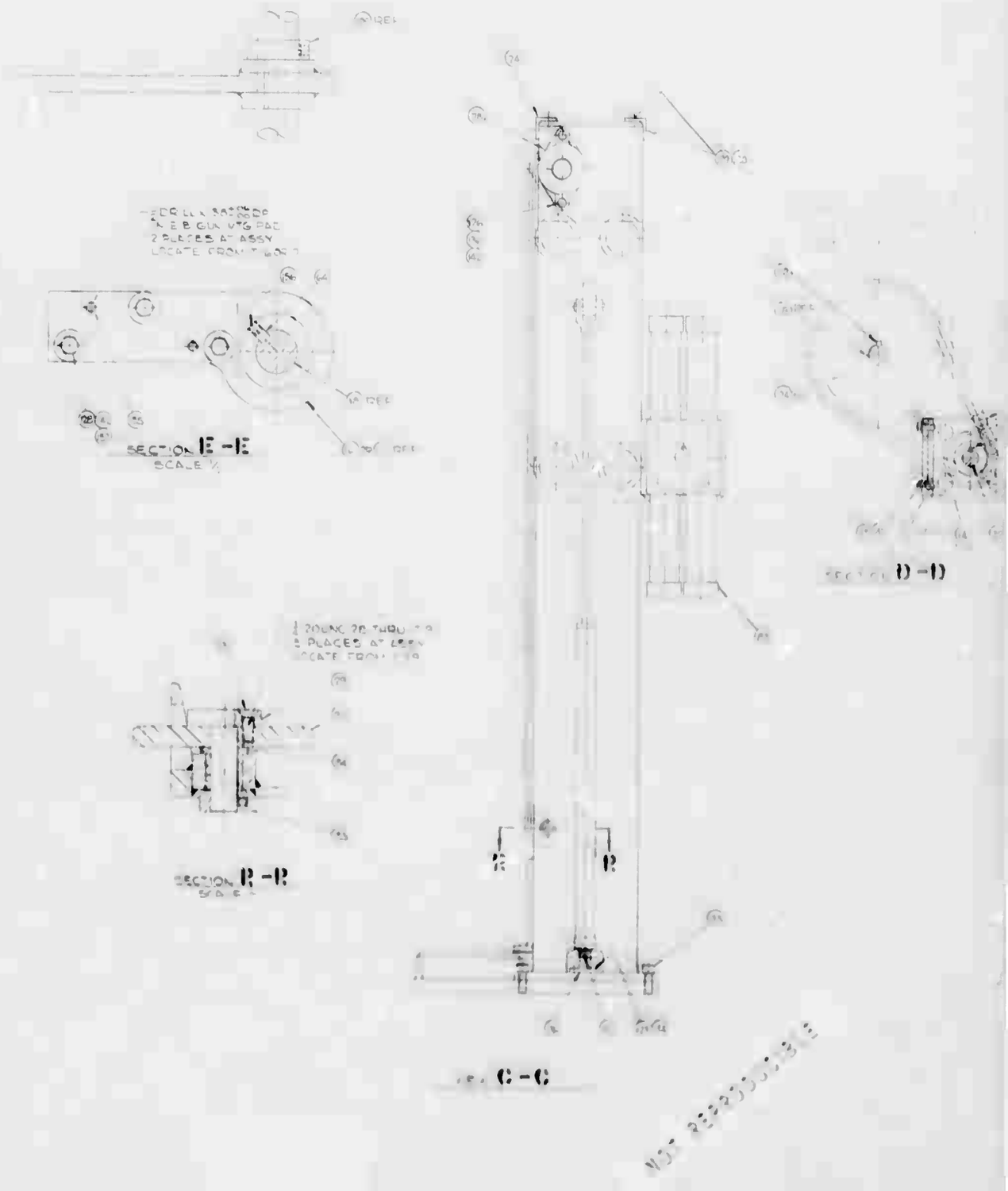
SECTION E-E
SCALE 1/1
SECTION D-D
SECTION B-B
SECTION C-C

B

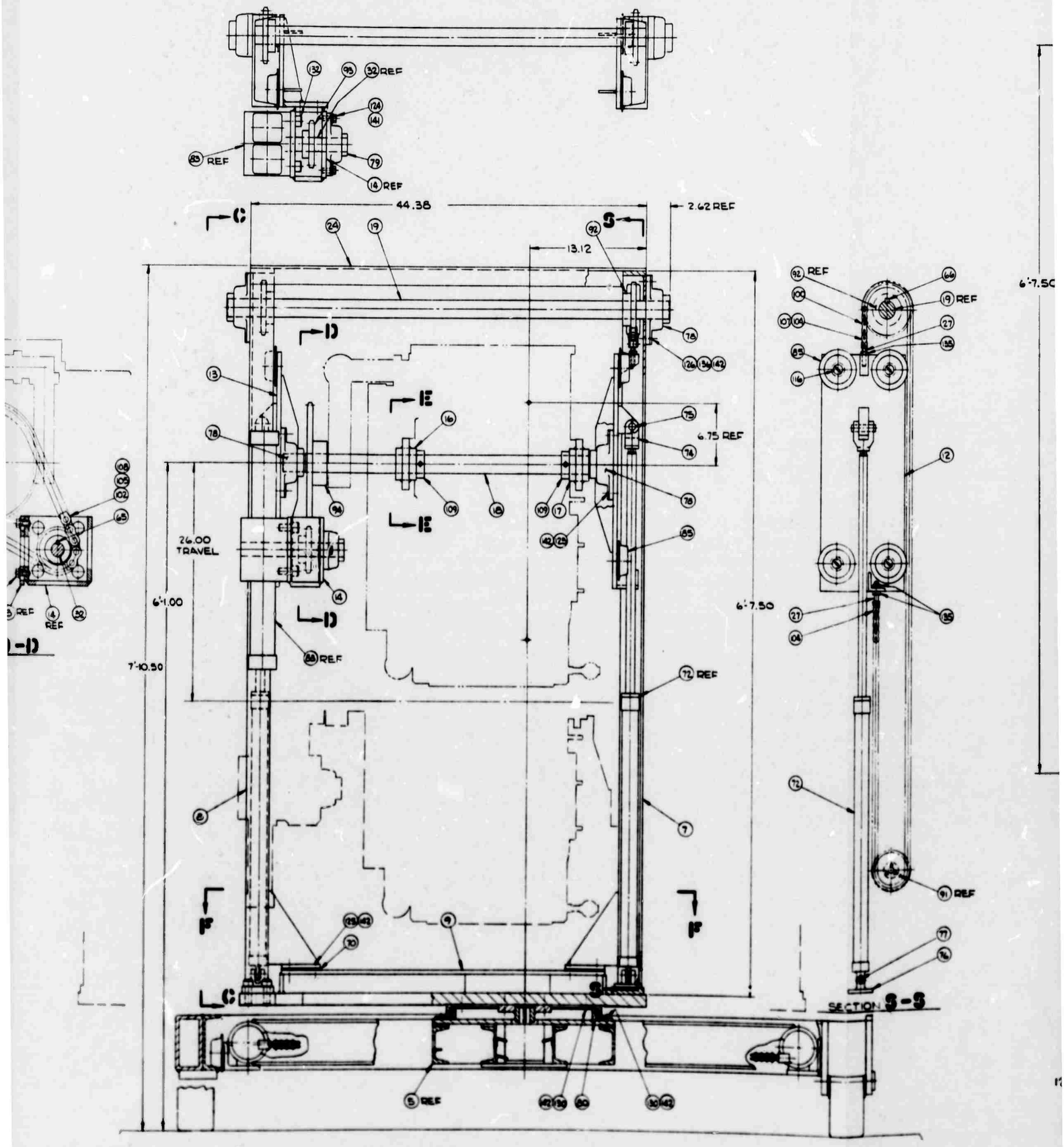

VIEW B-B
ROTATED 90° CCW

d

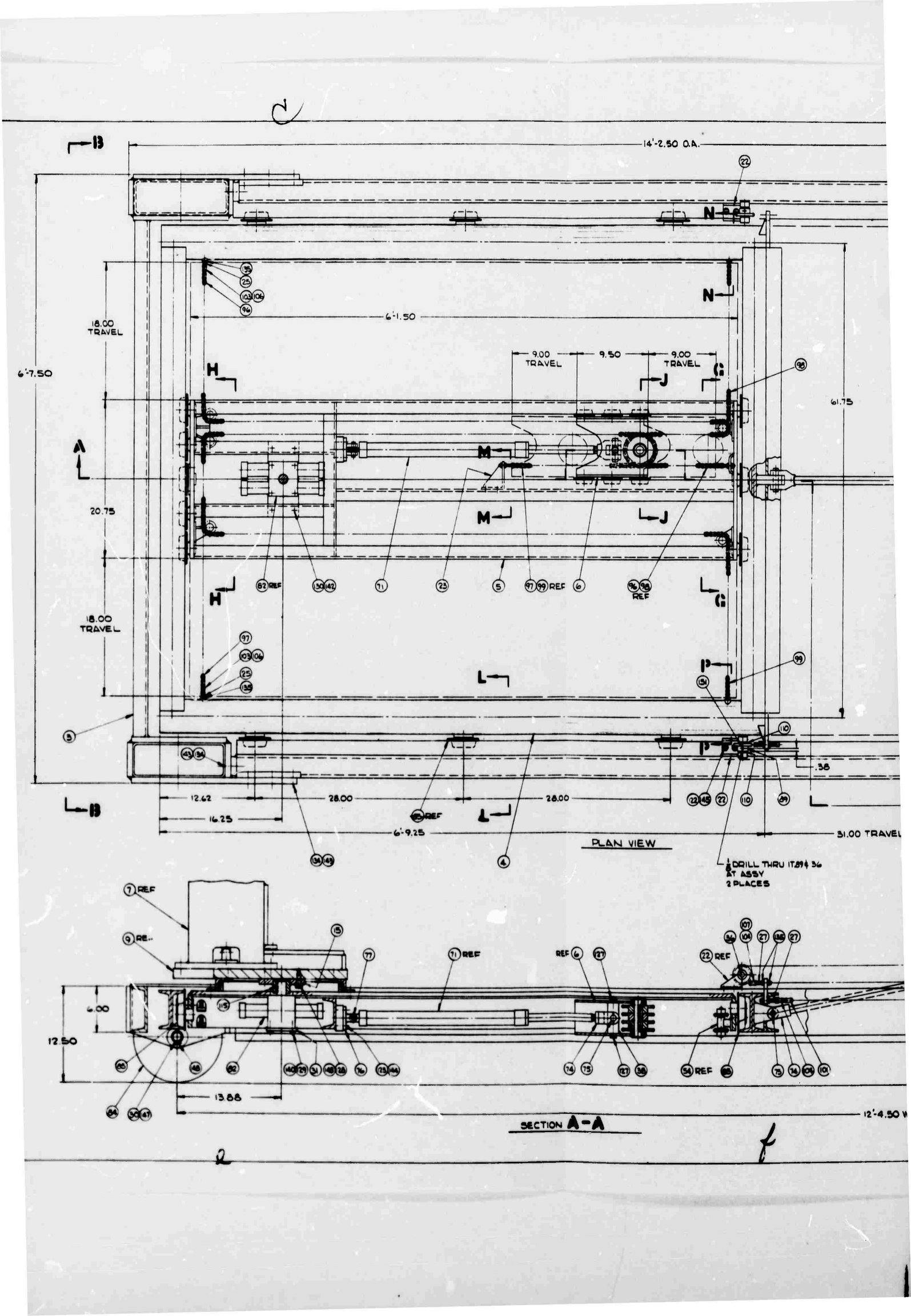
14'-2.50 O.A.
6'-1.50
18.00 TRAVEL
6'-7.50
9.00 TRAVEL
9.50
9.00 TRAVEL
61.75
20.75
18.00 TRAVEL
.38
12.62
28.00
28.00
16.25
6'-9.25
31.00 TRAVEL
PLAN VIEW
DRILL THRU IT.B94 36 AT ASSY 2 PLACES
6.00
12.50
13.88
12'-4.50
SECTION A-A

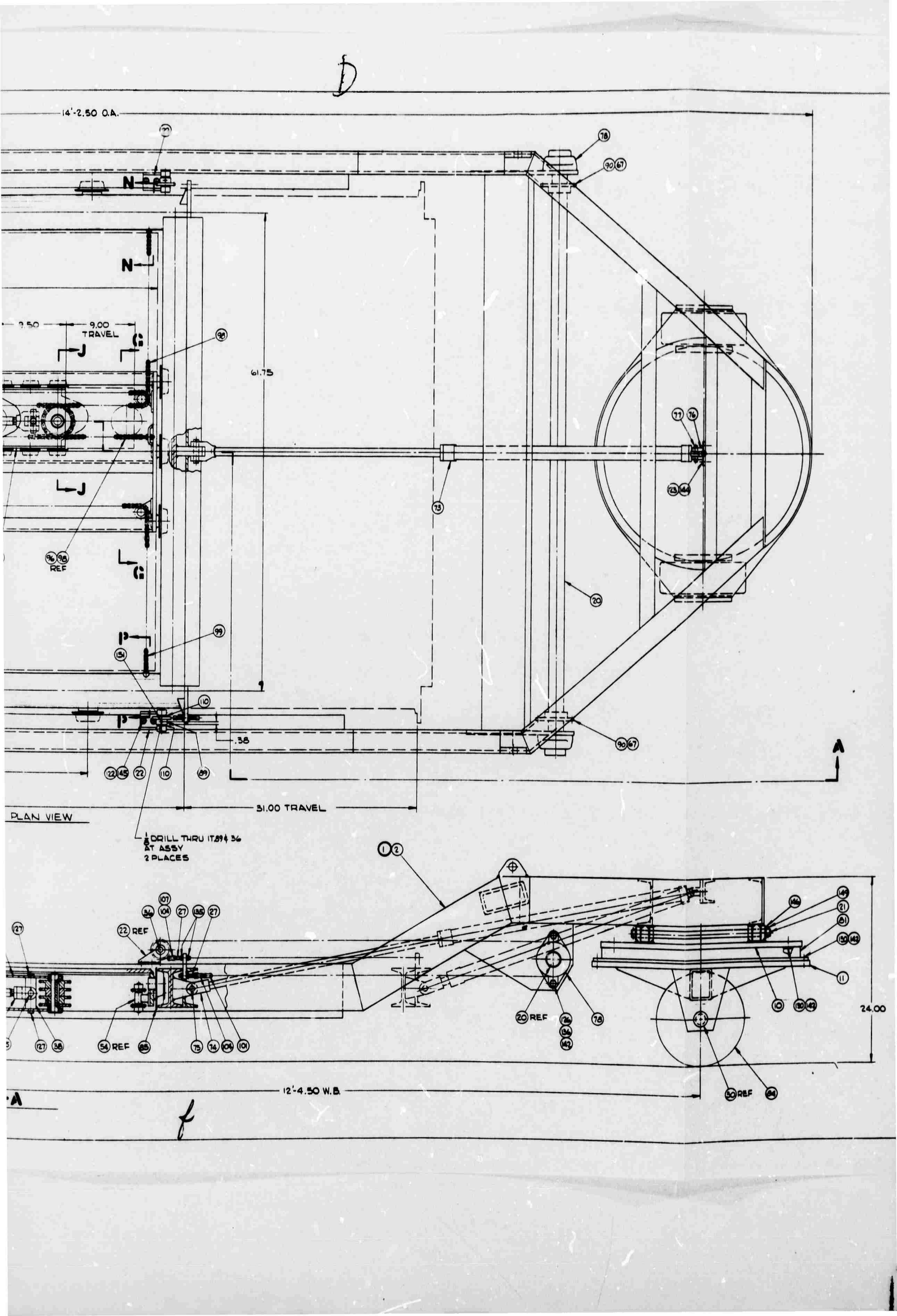
14'-2.50 O.A.
9.00 TRAVEL
61.75
.38
31.00 TRAVEL
PLAN VIEW
DRILL THRU 17.89 & 36 AT ASSY 2 PLACES
24.00
12'-4.50 W.B.
REF

E

A

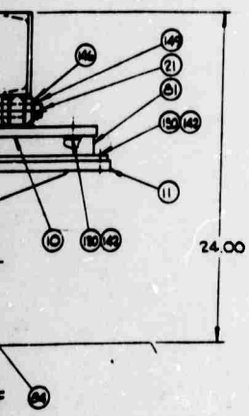

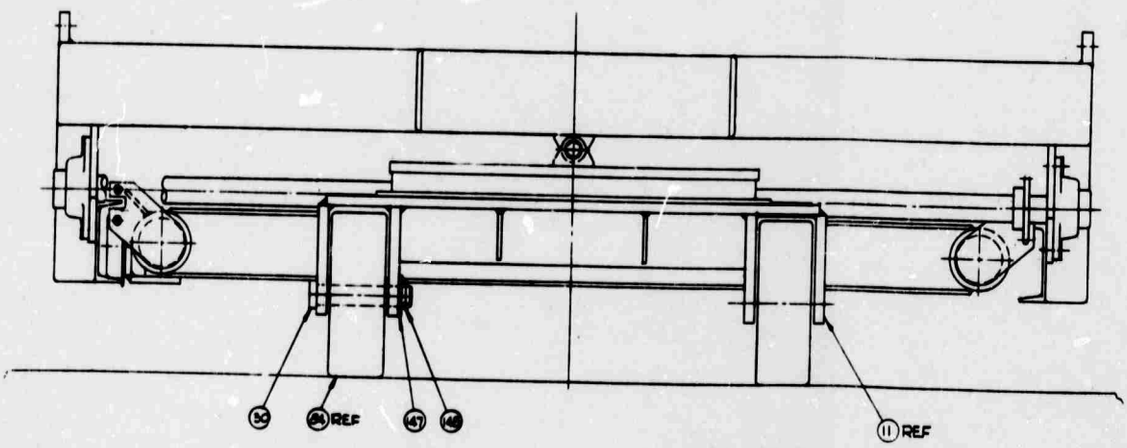

9

F

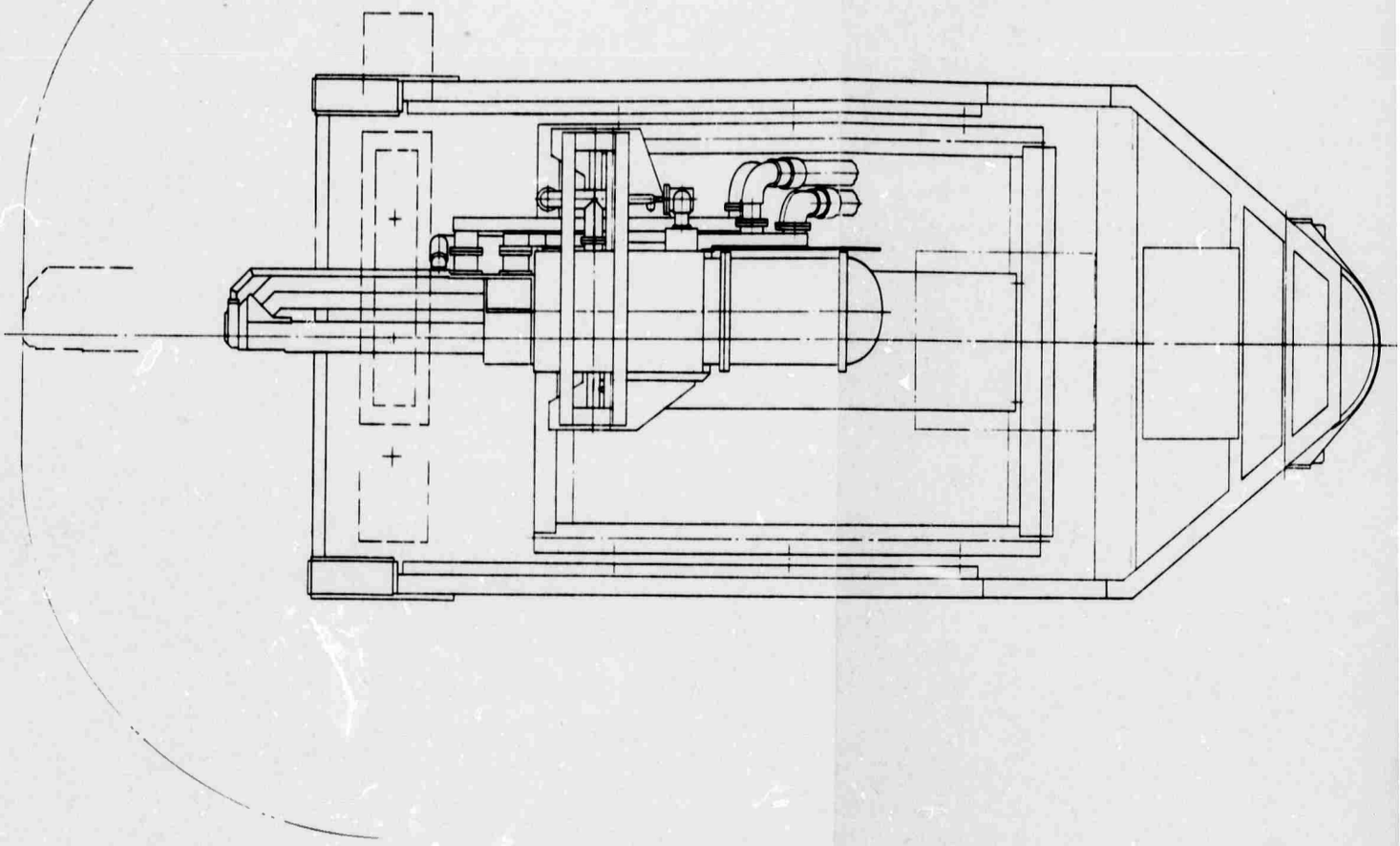

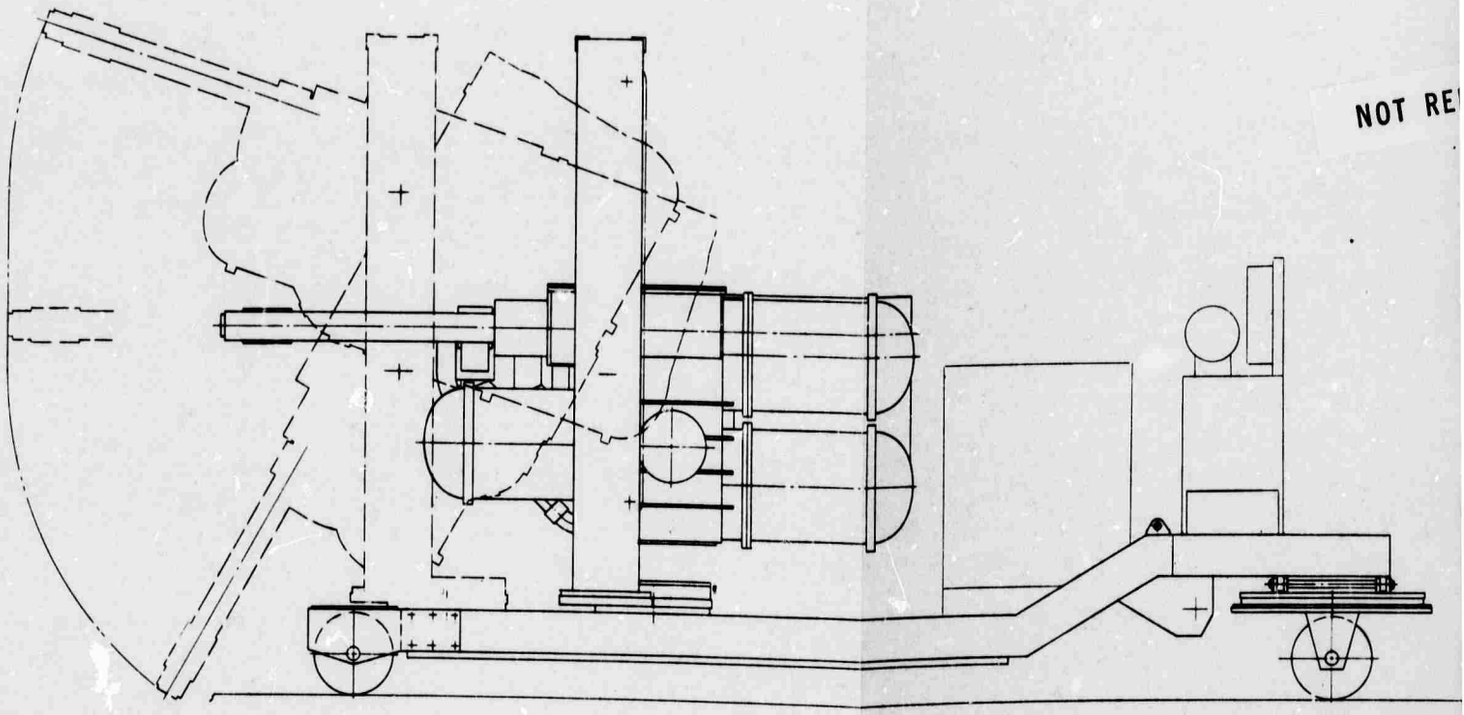

NOT RE

L

G

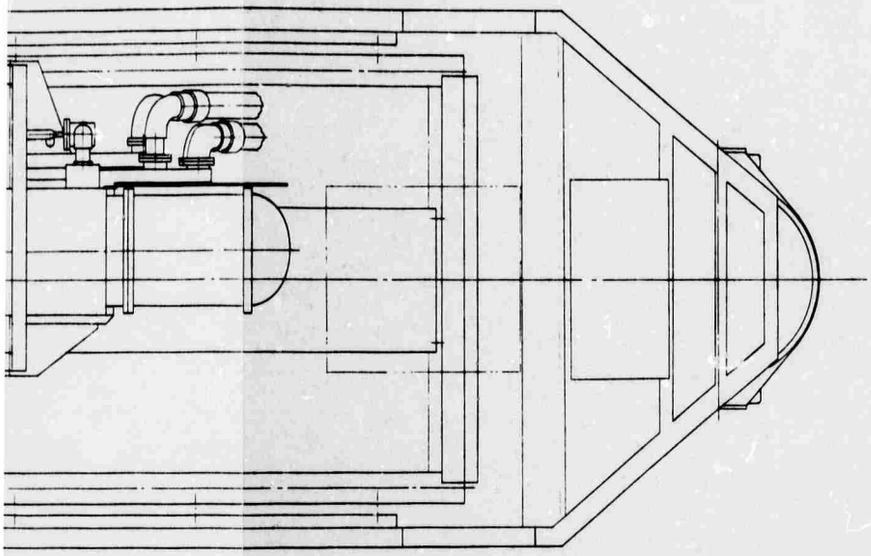

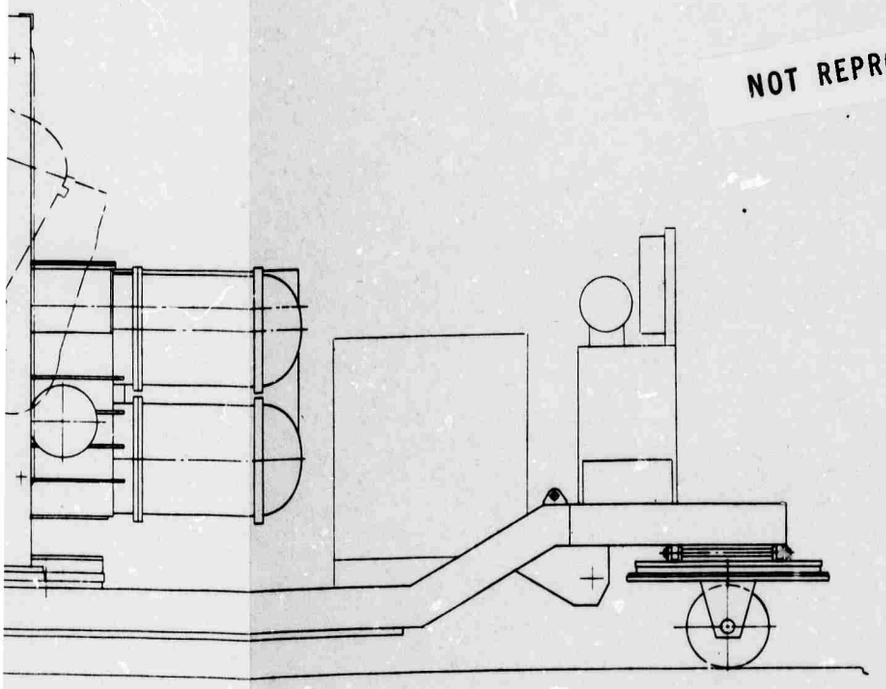

944J687

a

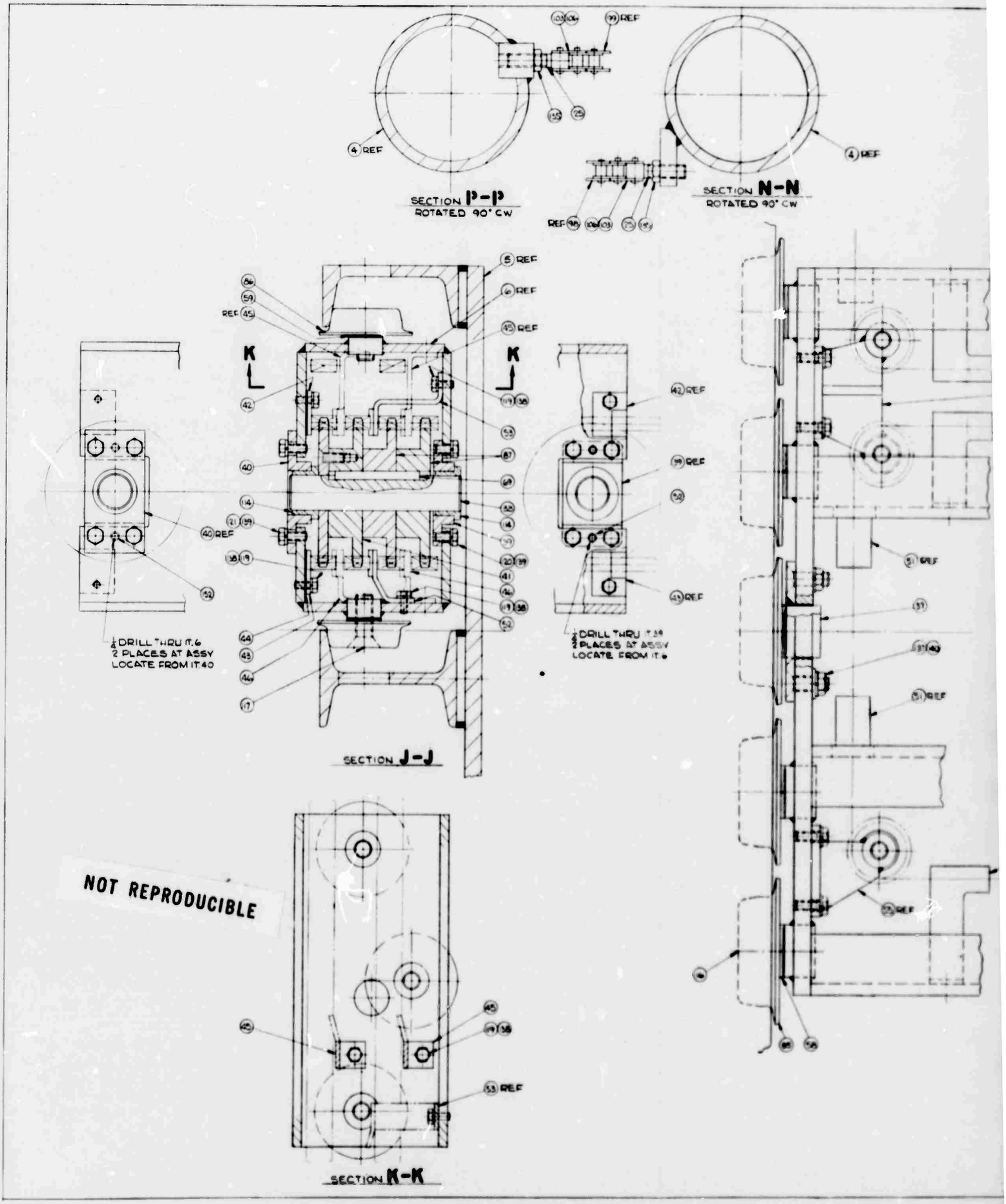

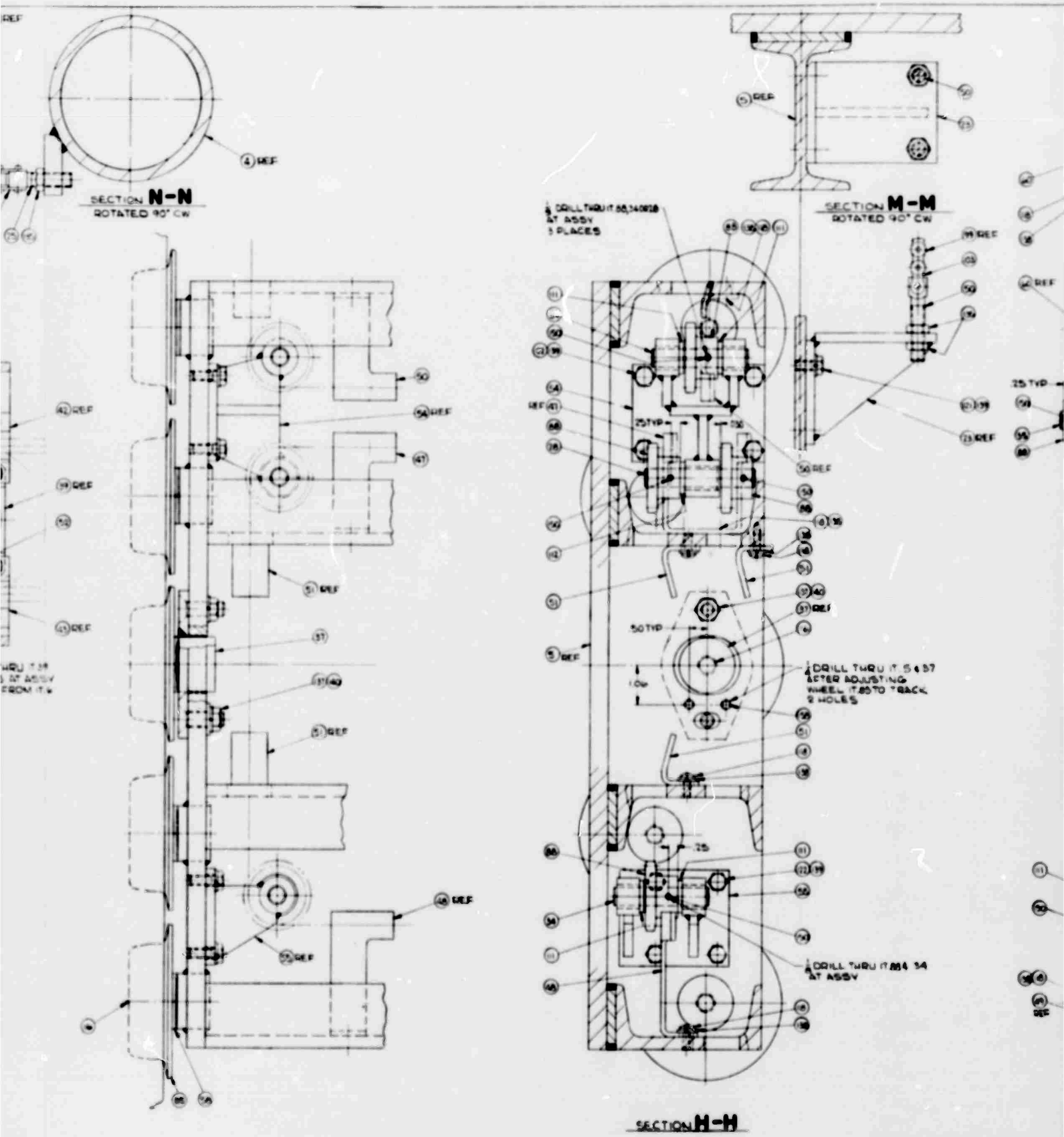
SECTION N-N
ROTATED 90° CW
SECTION M-M
ROTATED 90° CW
DRILL THRU IT 88,140,138 AT ASSY 3 PLACES
DRILL THRU IT 5 & 37 AFTER ADJUSTING WHEEL IT 85 TO TRACK 2 HOLES
DRILL THRU IT 84 & 14 AT ASSY
SECTION H-H

C

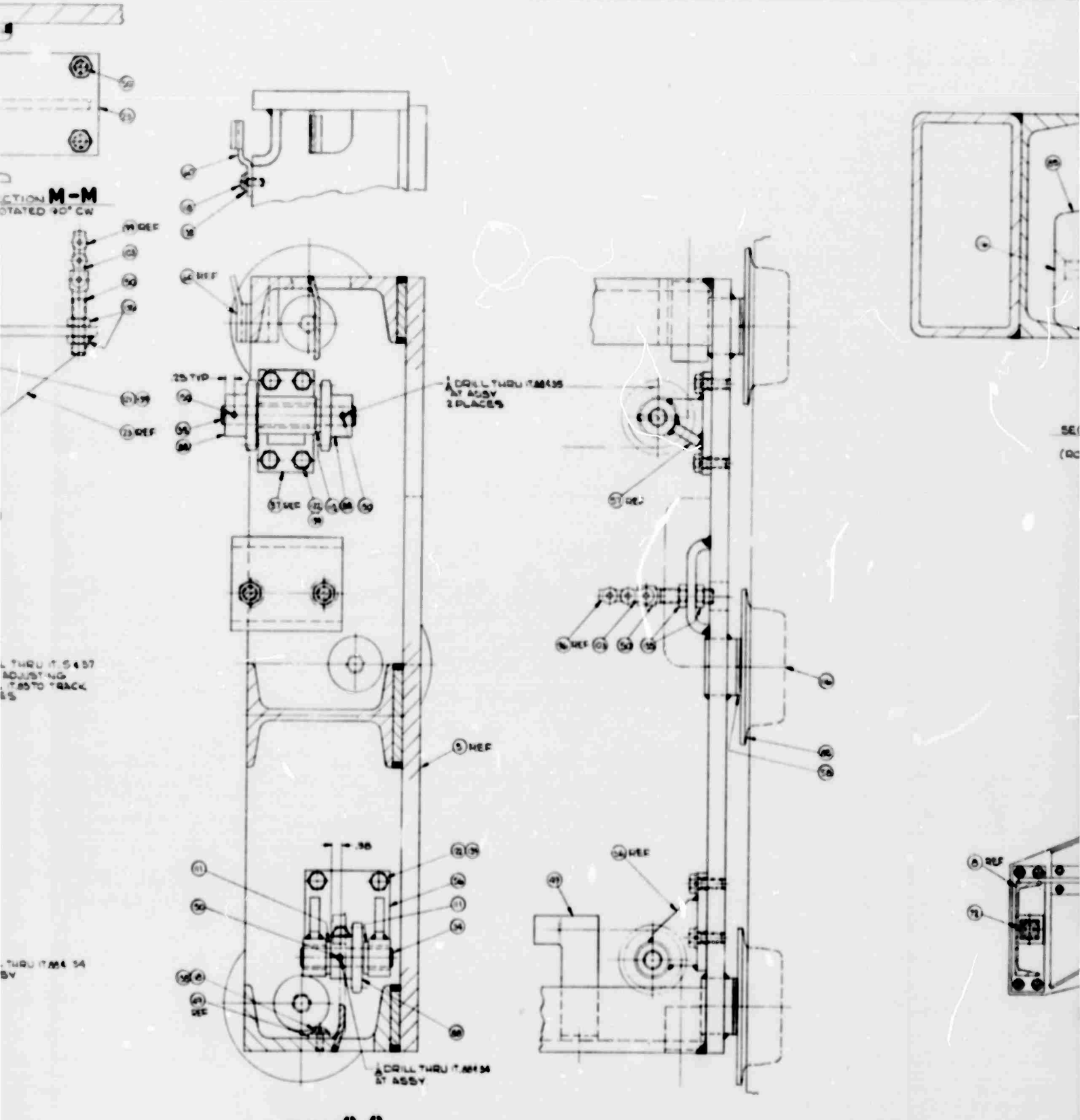
SECTION M-M
ROTATED 90° CW
.25 TYP
DRILL THRU .M4 .35
AT ASSY
2 PLACES
REF
DRILL THRU .M4 .34
AT ASSY

SECTION G G

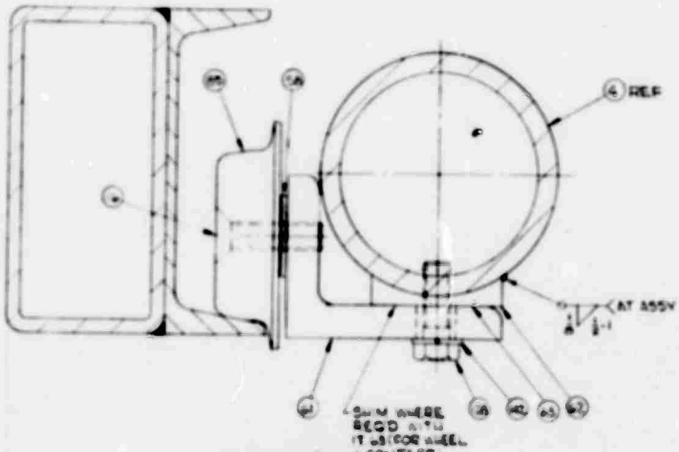

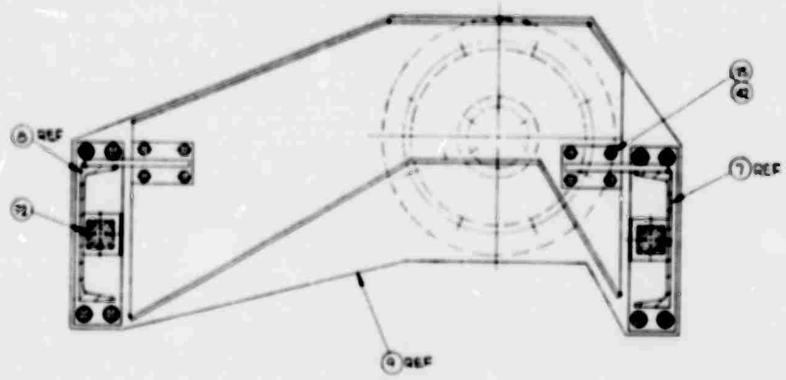

APPENDIX B

REFERENCES

REFERENCES

1. B. W. Schumacher, "Electron Beam Cutting of Rocks and Concrete" in: Electron and Ion Beam Science and Technology, Third International Conference, R. A. Bakish, Ed.; The Electrochemical Society Inc. New York 1968, pp. 447-468. Also E/MJ, June 1969, pp. 116-119.

2. Rock Breakage by Means of Electron Beam Piercing (Laboratory Tests) B. W. Schumacher and C. R. Taylor, Record of 10th Symposium on Electron, Ion, and Laser Beam Technology (L. Marton, ed.); San Francisco Press, Inc., 1969; pp. 271-284.

3. Westinghouse Brochure B-9604. (Available from Westinghouse Industrial Equipment Division, P.O. Box 300, Sykesville, Md. 21784.)

4. J. Lempert, The Nonvacuum Electron Beam Welder as a Welding Tool, IEEE Electric Welding Conf., Nov. 15-17, 1966, Detroit, Michigan.

5. Donald C. Ross, "Quartz Gabbro and Anorthositic Gabbro: Markers of Offset Along the San Andreas Fault in the California Coast Range," Bulletin of Geological Society of America, Vol. 81 (Dec. 1970), pp. 3647-3662.

6. B. W. Schumacher, "Power Density Limits for the Particle Penetration Laws and the Onset of Energy Phenomena in Electron Beam Targets" in: Electron and Ion Beam Science and Technology, Third International Conference, R. A. Bakish, Ed.; The Electrochemical Society, Inc., New York, 1968, pp. 74-93.

7. J. D. Jackson, Classical Electrodynamics, John Wiley & Sons, New York 1962, Chapter 13.

8. B. W. Schumacher, "A Review of the (Macroscopic) Laws for the Electron Penetration Through Matter;" in "First International Conference on Electron and Ion Beam Science and Technology;" R. Bakish, Editor; Wiley and Sons, New York, 1965.

9. "Electron Beams as Tools," Westinghouse Scientific Paper 71-1C2-EWELD-P1, B. W. Schumacher, (Available from the author.)